# Dynamic Soil Reactions in Radially Non-Homogeneous Soil Media

AUTHOR(S):

LAKSHMANAN, Narayanan; MINAI, Ryoichiro

# Dynamic Soil Reactions in Radially Non-Homogeneous Soil Media

By Narayanan LAKSHMANAN and Ryoichiro MINAI

(Manuscript received March 27, 1981)


## Abstract

Studies on soil structure interaction have been attracting the attention of research workers for the last two decades. Workable estimates of the complex stiffnesses under plane-strain conditions in homogeneous media have been provided by Prof. M. Novak. However, due to many reasons the soil may possess lesser values for the complex Lamé's constants, namely $\lambda$ and $G$, near the pile location.

Analytical formulations, using Whittaker's functions have been presented for the four important loading cases encountered in piles, namely vertical, torsional, rocking and horizontal. The behaviour of the complex stiffnesses, as indicated by their real and imaginary parts, with the non-dimensional frequency parameter $a_0^*(=\omega r_0/v_s)$ has been discussed and relevant conclusions drawn.


## 1. Introduction

Pile foundations are extensively used for supporting many civil engineering structures. Many of these are exposed to dynamic loading. Some of the structures subjected to dynamic loading, and which are supported on piles are (i) high rise buildings, tall towers and chimney stacks which are exposed to the dynamic action of wind and seismic loading; (ii) off-shore installations subjected to the action of wave, current and wind forces; and (iii) machine foundations, particularly turbo generator pedestals and nuclear power plant structures. When these foundations are exposed to oscillatory loads, the pile interacts with the soil. Because of their importance, the studies on soil-pile interaction have attracted the attention of many scientists over the last two decades.[1 to 11] Prof. M. Novak[2] has shown that good estimates for soil-pile interaction, and the resultant soil reactions can be obtained using the plane-strain approximation. However the plane-strain models tend to give higher values of stiffness when compared with experimental results. Hence Prof. Novak[3] has suggested an annular ring of soil around the pile, having different visco-elastic soil properties compared to the elastic half space. The reasons for considering a soil ring having lower elastic moduli are many fold. Some of them can be listed as (i) the soil structure being disturbed while the pile is installed in place; (ii) the higher magnitudes of stresses in the vicinity of the pile, and the resultant reduction in the tangential elastic moduli due to the

non-linear soil behaviour. This phenomenon causes wave propagation to occur in a non-homogeneous soil medium; and (iii) the high level of oscillations and resultant fatigue may affect the soil properties in the near vicinity of the pile. As the plane-strain approximation has produced workable estimates of the soil reactions, a similar approach for non-homogeneous soil medium under different loading cases is attempted. The soil is considered visco-elastic, and its preperties vary along a radial line.

## 2. Soil Reactions under Vertical Vibrations

The assumptions that are made are (i) the radial and tangential displacements are very small in comparison to the vertical displacement and hence can be neglected. That is $u=v=0$, and also the variation of vertical displacement with depth is not considered. Consider a unit thickness of soil-pile system as shown in **Fig. 1.**

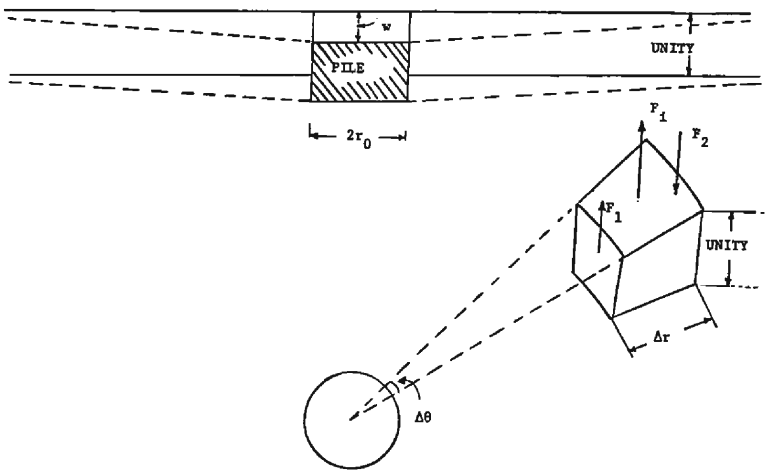


Fig. 1 Vertical displacement in soil layer.

Let $G_\infty$ be the complex shear modulus of the soil as the radial distance tends to infinity from the centre of the pile. Let $G(r)$ be the complex shear modulus at a distance, $r$ from the centre of the pile. Consider now the equilibrium of the element shown in **Fig. 1.**

$$F_1=-G(r)\frac{\partial w}{\partial r}\cdot r\Delta\theta \qquad \cdots\cdots(1)$$

$$F_2=\left\{G(r)+\frac{dG(r)}{dr}\cdot\Delta r\right\}\left\{\frac{\partial w}{\partial r}+\frac{\partial}{\partial r}\left(\frac{\partial w}{\partial r}\right)\cdot\Delta r\right\}(r+\Delta r)\,\Delta\theta \qquad \cdots\cdots(2)$$

and the inertial force $F_i$ is given by

$$F_i=-\rho(r\Delta\theta\Delta r)\frac{\partial^2 w}{\partial t^2} \qquad \cdots\cdots(3)$$

Hence by considering the equilibrium of forces $F_1$, $F_2$ and $F_i$ the following equation is obtained:

$$-G(r)\frac{\partial w}{\partial r}\cdot r\Delta\theta+\left[G(r)+\frac{dG(r)}{dr}\cdot\Delta r\right]\left[\frac{\partial w}{\partial r}+\frac{\partial}{\partial r}\left(\frac{\partial w}{\partial r}\right)\cdot\Delta r\right](r+\Delta r)\Delta\theta$$
$$=\rho(r\Delta\theta\Delta r)\frac{\partial^2 w}{\partial t^2} \qquad \cdots\cdots(4)$$

Dividing throughout by $r\Delta\theta\Delta r$, and neglecting higher order terms yields

$$G(r)\frac{\partial^2 w}{\partial r^2}+\left[\frac{dG(r)}{dr}+\frac{G(r)}{r}\right]\frac{\partial w}{\partial r}=\rho\frac{\partial^2 w}{\partial t^2} \qquad \cdots\cdots(5)$$

Under harmonic excitation

$$w=\bar{w}e^{i\omega t} \qquad \cdots\cdots(6)$$

equation (5) can be rewritten as

$$G(r)\frac{\alpha^2\bar{w}}{dr^2}+\left[\frac{dG(r)}{dr}+\frac{G(r)}{r}\right]\frac{d\bar{w}}{dr}=i^2\omega^2\rho\bar{w} \qquad \cdots\cdots(7)$$

At this stage, the following transformations and parameters are introduced.

$$\xi=r/r_0 \qquad \cdots\cdots(8)$$

$$G(r)=G_\infty\cdot g(\xi) \qquad \cdots\cdots(9)$$

$$G_\infty=G_s(1+iD_s) \qquad \cdots\cdots(10)$$

$$s^2=\frac{i^2\omega^2\rho}{G_\infty} \qquad \cdots\cdots(11)$$

$$a_0=sr_0 \qquad \cdots\cdots(12)$$

$$\Phi(\xi)=\bar{w}(r)/\bar{w}(r_0) \qquad \cdots\cdots(13)$$

where $G_s$ and $D_s$ are the shear modulus and material damping factor of the soil, respectively, at infinity. Hence equation (7) reduces to

$$\left[g\frac{d^2}{d\xi^2}+\left(\frac{g}{\xi}+g'\right)\frac{d}{d\xi}-a_0^2\right]\Phi=0 \qquad \cdots\cdots(14)$$

Let $$\Phi(\xi)=\eta(\xi)\cdot\psi(\xi) \qquad \cdots\cdots(15)$$

Hence $$\frac{d\Phi}{d\xi}=\eta\psi'+\psi\eta' \qquad \cdots\cdots(16)$$

and $$\frac{d^2\Phi}{d\xi^2}=\eta''\psi+2\eta'\psi'+\psi''\eta \qquad \cdots\cdots(17)$$

where the primes indicate differentiation with respect to $\xi$. Equation (14) now becomes

$$g(\eta''\phi+2\eta'\phi'+\phi''\eta)+\left(\frac{g}{\xi}+g'\right)(\eta\phi'+\phi\eta')-a_0^2\cdot\phi\eta=0 \qquad \cdots\cdots(18)$$

Dividing throughout by $g\eta$ and rearranging yields

$$\left[\frac{d^2}{d\xi^2}+\left(\frac{2\eta'}{\eta}+\frac{g'}{g}+\frac{1}{\xi}\right)\frac{d}{d\xi}+\left(\frac{\eta''}{\eta}+\frac{\eta'}{\eta}\cdot\frac{1}{\xi}+\frac{g'}{g}\cdot\frac{\eta'}{\eta}-\frac{a_0^2}{g}\right)\right]\phi=0 \qquad \cdots\cdots(19)$$

The Whittaker's equation[12),13)], to which analytical solutions are feasible, can be written as

$$\left[\frac{d^2}{d\epsilon^2}+\left\{-\frac{1}{4}+\frac{\chi}{\epsilon}-\frac{\left(\mu^2-\frac{1}{4}\right)}{\epsilon^2}\right\}\right]W_{\chi,\mu}(\epsilon)=0 \qquad \cdots\cdots(20)$$

By assuming that $\epsilon=\epsilon(\xi)$ equation (20) can be transformed to

$$\left[\frac{d^2}{d\xi^2}-\frac{\epsilon''}{\epsilon'}\frac{d}{d\xi}+(\epsilon')^2\left\{-\frac{1}{4}+\frac{\chi}{\epsilon}-\frac{\left(\mu^2-\frac{1}{4}\right)}{\epsilon^2}\right\}\right]W_{\chi,\mu}[\epsilon(\xi)]=0 \qquad \cdots\cdots(21)$$

The comparison of equations (19) with (21) yields

$$\frac{2\eta'}{\eta}+\frac{g'}{g}+\frac{1}{\xi}=-\frac{\epsilon''}{\epsilon'} \qquad \cdots\cdots(22)$$

$$\frac{\eta''}{\eta}+\frac{\eta'}{\eta}\left(\frac{g'}{g}+\frac{1}{\xi}\right)-\frac{a^2}{g}=(\epsilon')^2\left[-\frac{1}{4}+\frac{\chi}{\epsilon}-\frac{\left(\mu^2-\frac{1}{4}\right)}{\epsilon^2}\right] \qquad \cdots\cdots(23)$$

Integrating equation (22) with respect to $\xi$ gives

$$\eta=\frac{C_0}{\sqrt{g\xi\epsilon'}} \qquad \cdots\cdots(24)$$

The substitution of $\eta$ as given in (24) into equation (23) yields

$$2\frac{\epsilon'''}{\epsilon'}-3\left(\frac{\epsilon''}{\epsilon'}\right)^2+\left(\frac{\epsilon'}{\epsilon}\right)^2(-\epsilon^2+4\chi\epsilon-4\mu^2+1)$$
$$=-\frac{4a_0^2}{g}-\frac{2g''}{g}+\left(\frac{g'}{g}\right)^2+\frac{1}{\xi^2}-\left(\frac{2g'}{g}\right)\left(\frac{1}{\xi}\right) \qquad \cdots\cdots(25)$$

The solution $\epsilon(\xi)$ to the above equation togther with equation (24) may give the solution to equation (14) in terms of Whittaker's functions $W\chi,\ \mu$.[12)] For the sake of simplicity, it is assumed tere that

$$g=c\xi \qquad \cdots\cdots(26)$$

and that $(\epsilon')^2=4a_0^2/g$ $\cdots\cdots(27)$

At this stage it is postulated that there are two distinct regions in the soil medium. The first one, an inner ring, whose one face is in contact with the pile. The outer

face of the above ring is in contact with a homogeneous soil medium having an elastic shear modulus $G_s$. The value of $\xi$ being equal to unity implies the pile-soil interface, where the elastic shear modulus is given by $c\ G_s$, as can be deduced from equations (9) and (26). The modified radial co-ordinate $\xi$, corresponding to the interface of the inner non-homogeneous soil ring and outer homogeneous soil medium, has a value equal to $(1/c)$.

From equations (26) and (27) the value of $\epsilon$ can be obtained as

$$\epsilon=4a_0\sqrt{\xi/c} \qquad \cdots\cdots(28)$$

By substituting equations (26), (27) and (28) into equation (25), and assuming $\chi=0$, the value of $\mu$ can be solved as $\pm 1$. The solutions to Whittaker's equation are given below.

$$M_{\chi,\mu}(\epsilon)=e^{-(\epsilon/2)}\cdot\epsilon^{(1/2+\mu)}\cdot M\left(\frac{1}{2}+\mu-\chi,\ 1+2\mu,\ \epsilon\right) \qquad \cdots\cdots(29)$$

$$W_{\chi,\mu}(\epsilon)=e^{-(\epsilon/2)}\cdot\epsilon^{(1/2+\mu)}\cdot U\left(\frac{1}{2}+\mu-\chi,\ 1+2\mu,\ \epsilon\right) \qquad \cdots\cdots(30)$$

$$W_{\chi,\mu}(\epsilon)=\frac{\Gamma(-2\mu)}{\Gamma\left(\frac{1}{2}-\mu-\chi\right)}\cdot M_{\chi,\mu}(\epsilon)+\frac{\Gamma(2\mu)}{\Gamma\left(\frac{1}{2}+\mu-\chi\right)}\cdot M_{\chi,-\mu}(\epsilon) \qquad \cdots\cdots(31)$$

When

$$\chi=0,\quad M_{0,\mu}=M_{0,-\mu} \qquad \cdots\cdots(32)$$

$$M\left(\frac{1}{2}+\mu,\ 1+2\mu,\ 2z\right)=\Gamma(1+\mu)\cdot e^{z}\cdot\left(\frac{z}{2}\right)^{-\mu}\cdot I_{\mu}(z) \qquad \cdots\cdots(33)$$

and

$$U\left(\frac{1}{2}+\mu,\ 1+2\mu,\ 2z\right)=\pi^{-1/2}\cdot e^{z}\cdot(2z)^{-\mu}\cdot K_{\mu}(z) \qquad \cdots\cdots(34)$$

where $\Gamma$, $I_\mu$ and $K_\mu$ are gamma function, the $\mu$th order modified Bessel functions of the first and second kinds, respectively.

By using the relations given in equations (29) through (34), the solutions for $\Phi(\xi)$ can be derived as

$$\Phi(\xi)=\frac{1}{\sqrt{c\xi}}\left[AI_1(z)+BK_1(z)\right] \qquad \cdots\cdots(35)$$

where $z=\epsilon/2=2a_0\sqrt{\xi/c}$

To obtain the complex pile-soil stiffness, a unit vertical displacement is given to the pile, and perfect bond between pile and soil is assumed. The value of $\xi$ being unity at the pile-soil interface results in the following equations:

$$AI_1(z_0)+BK_1(z_0)=\sqrt{c} \qquad \cdots\cdots(36)$$

where $z_0=2a_0/\sqrt{c}$

The equations of plane-strain case are valid in the outer homogeneous soil medium. Hence by equating the displacement and the shear stress at the interface of the inner ring and outer homogeneous soil medium, two additional relations are obtained.

$$AI_1(z_1)+BK_1(z_1)=D_0K_0(a_0/c) \qquad \cdots\cdots(37)$$

$$A[-cI_1(z_1)+a_0I_0(z_1)]-B[cK_1(z_1)+a_0K_0(z_1)]=-D_0a_0K_1(a_0/c) \qquad \cdots\cdots(38)$$

where $z_1=2a_0/c$

The values of $A$, $B$ and $D_0$ can be solved from equations (36), (37) and (38). Once $A$ and $B$ are known the vertical stiffness of soil per unit length of cylinder can be easily computed using the relation.

$$k_w=-2\pi cG_\infty r_0\left(\frac{d\Phi}{dr}\right)_{r=r_0}=(S_{w1}+iS_{w2})G_s \qquad \cdots\cdots(39)$$

Equation (39) is in the same format as given in Ref. 2. **Fig. 2** and **Fig. 3** show the variation of $S_{w1}$ and $S_{w2}$ with varying values of $c$, and the non-dimensional frequency parameter $a_0^*(=\omega r_0/v_s\ ;\ v_s=\sqrt{G_s/\rho})$. In these figures, the material damping factors $D_s$ are kept the same constant for both inner and outer media.

It is also possible to choose different material damping values in the inner ring as compared to the outer medium. **Fig. 4** and **Fig. 5** show the values of $S_{w1}$ and $S_{w2}$ for a material damping factor of 0.4 in the non-homogeneous medium and 0.1 in the outer homogeneous medium. The compatibility in this case will be achieved at a location where the real parts of elastic shear moduli are equal. However there will be a discontinuity in the imaginary parts of soil moduli. Another feasibility is to define the material damping factor as dependent on the value of $c$. That is when $c$ is small, a larger value of material damping can be defined. This simulates the condition that the larger non-homogeneous soil layer is association with higher stress and subsequent cracking, which in turn leads to a higher value for the material damping factor. A certain variation for material damping factor given by

$$D_R=0.1+(0.03/c)$$

has also been studied. **Fig. 6** and **Fig. 7** give the variations of $S_{w1}$ and $S_{w2}$ under such a condition.

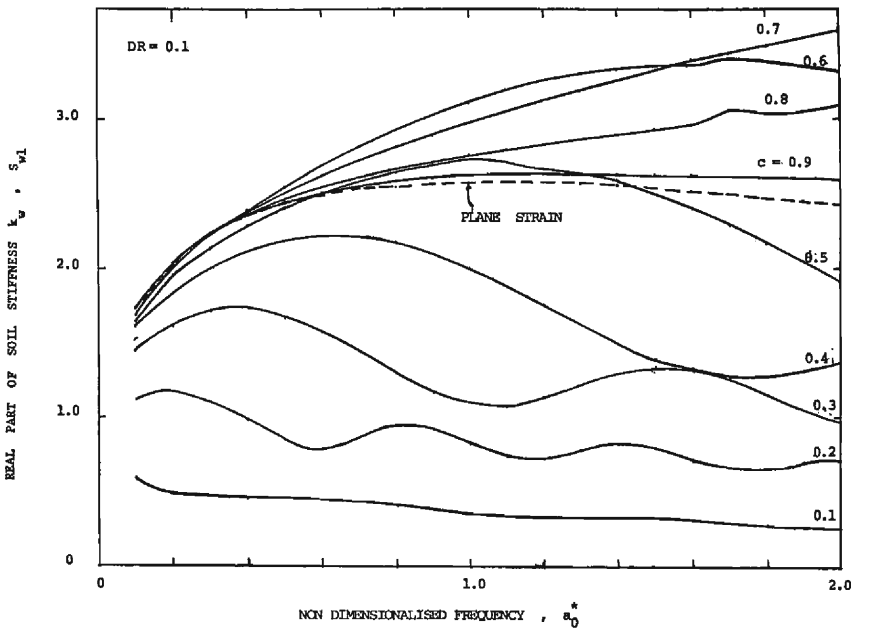


Fig. 2 Real part of soil stiffness in vertical direction.

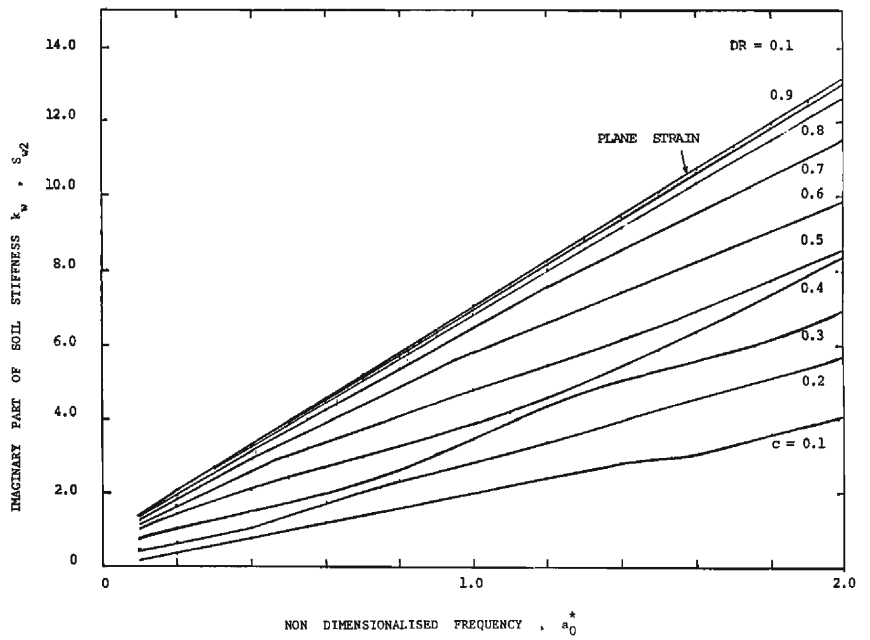


Fig. 3 Imaginary part of soil stiffness in vertical direction.

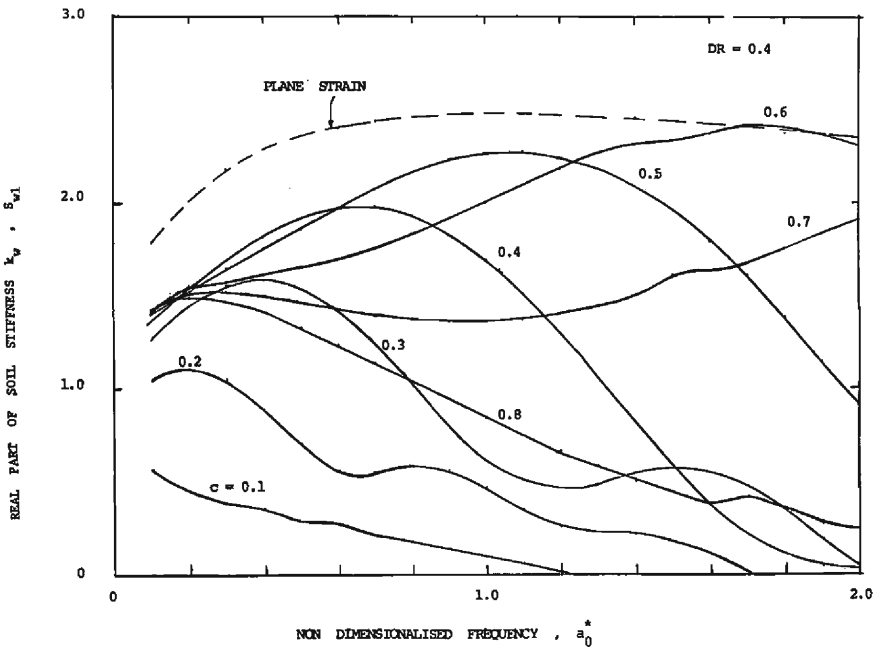


Fig. 4 Real part of soil stiffness in vertical direction.

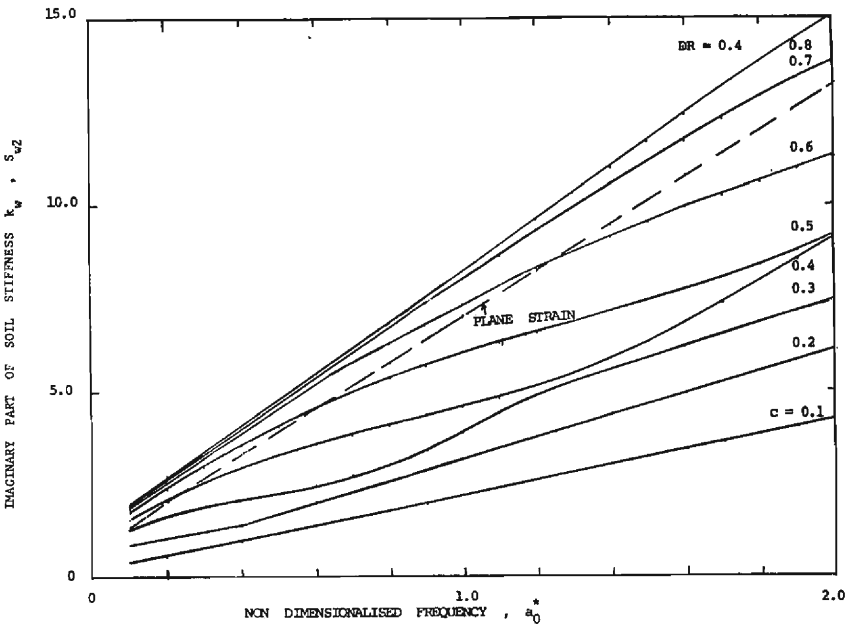


Fig. 5 Imaginary part of soil stiffness in vertical direction.

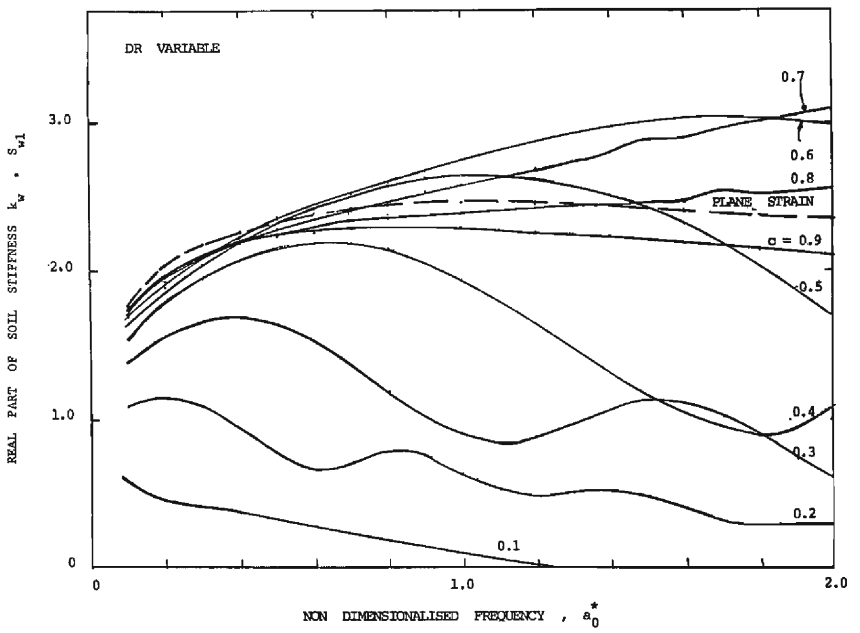


Fig. 6 Real part of soil stiffness in vertical direction.

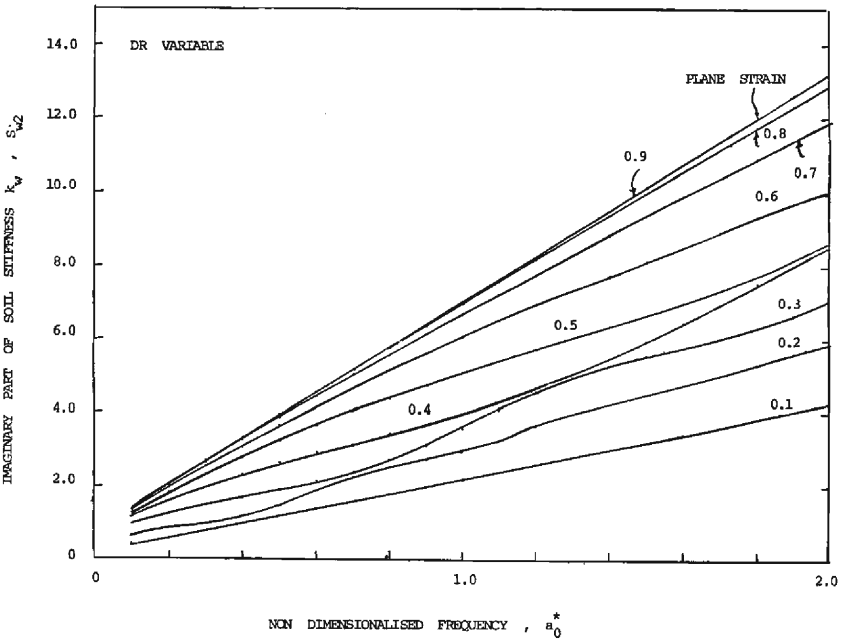


Fig. 7 Imaginary part of soil stiffness in vertical direction.

## 3. Soil Reactions under Torsional Vibrations

The assumptions that are made for the case of torsional vibration of the medium around the vertical axis of the cylinder are that the radial and vertical displacements are infinitesimally small and hence can be neglected. That is $u=w=0$. Variation of tangential displacement with depth is not considered. Consider the equilibrium of an element as shown in **Fig. 8.**

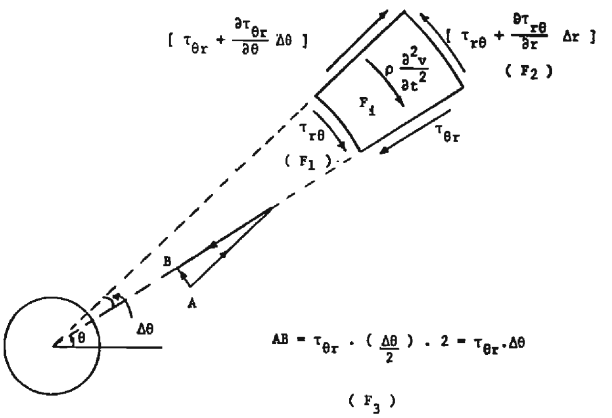


Fig. 8 Equilibrium of forces under torsion.

By considering the equilibrium of the element, the forces are

$$F_1=-G(r)\left(\frac{-v}{r}+\frac{\partial v}{\partial r}\right)\cdot r\Delta\theta$$

$$F_2=\left[G(r)+\frac{dG(r)}{dr}\cdot\Delta r\right]\left\{\left(\frac{-v}{r}+\frac{\partial v}{\partial r}\right)+\left(\frac{v}{r^2}-\frac{1}{r}\frac{\partial v}{\partial r}+\frac{\partial^2 v}{\partial r^2}\right)\Delta r\right\}(r+\Delta r)\cdot\Delta\theta$$

$$F_3=G(r)\left(\frac{-v}{r}+\frac{\partial v}{\partial r}\right)\Delta\theta\,\Delta r$$

$$F_i=-\rho(r\Delta\theta\,\Delta r)\frac{\partial^2 v}{\partial t^2}$$

By adding these and neglecting higher order terms the equilibrium equation can be written as

$$G(r)\left(\frac{\partial^2 v}{\partial r^2}+\frac{1}{r}\frac{\partial v}{\partial r}-\frac{v}{r^2}\right)+\frac{dG}{dr}\left(\frac{-v}{r}+\frac{\partial v}{\partial r}\right)=\rho\frac{\partial^2 v}{\partial t^2} \qquad \cdots\cdots(40)$$

With the substitutions given in equations (8) through (13) and by replacing $\Phi$ as $v(r)/v(r_0)$, equation (40) can be rewritten as

$$\left[g\frac{d^2}{d\xi^2}+\left(\frac{g}{\xi}+g'\right)\frac{d}{d\xi}-\left(\frac{g}{\xi^2}+\frac{g'}{\xi}\right)-a_0^2\right]\Phi=0 \qquad \cdots\cdots(41)$$

By adopting a similar procedure as explained in detail under the vertical vibations, and with $g=c\xi$, and $\chi=0$, the value of $\mu$ can be obtained as $\pm 3$, leading to the

expression for $\Phi$ as

$$\Phi(\xi) = \frac{1}{\sqrt{c\xi}} [AI_3(z) + BK_3(z)] \qquad \cdots\cdots(42)$$

where $z = 2a_0\sqrt{\xi/c}$

By proceeding exactly in the same fashion as for the vertical case three simultaneous equations can be set-up leading to the evaluation of $A$ and $B$. Then by applying unit rotation, that is $v = r_0$ at the soil pile interface the stiffness under torsion per unit rotation, per unit length of the pile can be evaluated as

$$k_\zeta = 2\pi G_\infty r_0^2 \Big[ -1.5\sqrt{c}\,\{AI_3(z_0) + BK_3(z_0)\} + a_0 \Big\{ A\Big(I_2(z_0) - \frac{3}{z_0} I_3(z_0)\Big) - B\Big(K_2(z_0) + \frac{3}{z_0} K_3(z_0)\Big)\Big\}\Big] \qquad \cdots\cdots(43)$$

That is

$$k_\zeta = G_s r_0^2 (S_{\zeta 1} + iS_{\zeta 2}) \qquad \cdots\cdots(44)$$

As in the case of vertical vibration three different cases have been studied, namely a) a constant material damping factor for both the inner non-homogeneous ring and the outer homogeneous soil medium, b) a constant but different, and higher material damping factor for the inner ring as compared to the outer medium and c) a ring thickness-dependent material damping factor.

The real and imaginary parts of the soil stiffness represented by $S_{\zeta 1}$ and $S_{\zeta 2}$ under torsion are plotted in **Fig. 9** to **Fig. 14**.

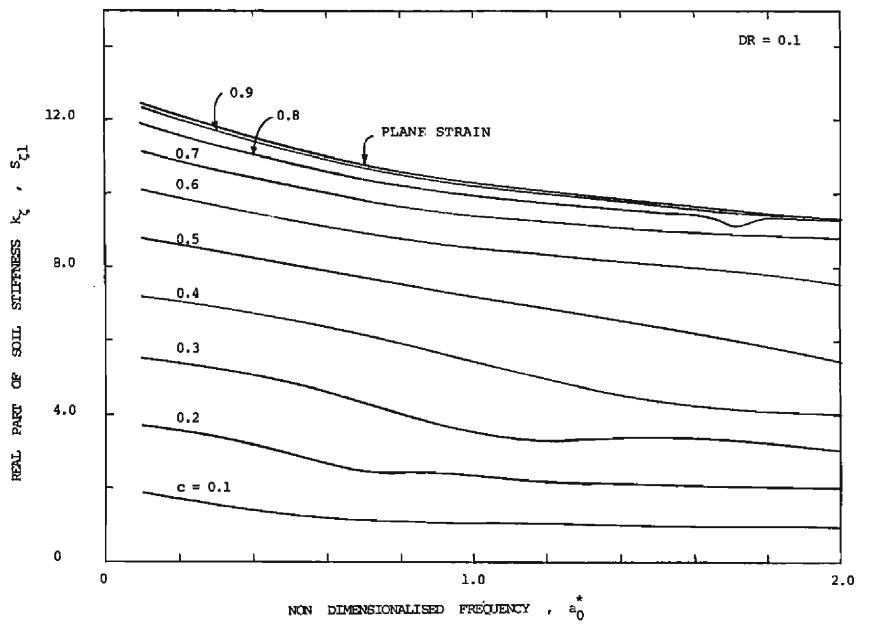


Fig. 9 Real part of soil stiffness in torsion.

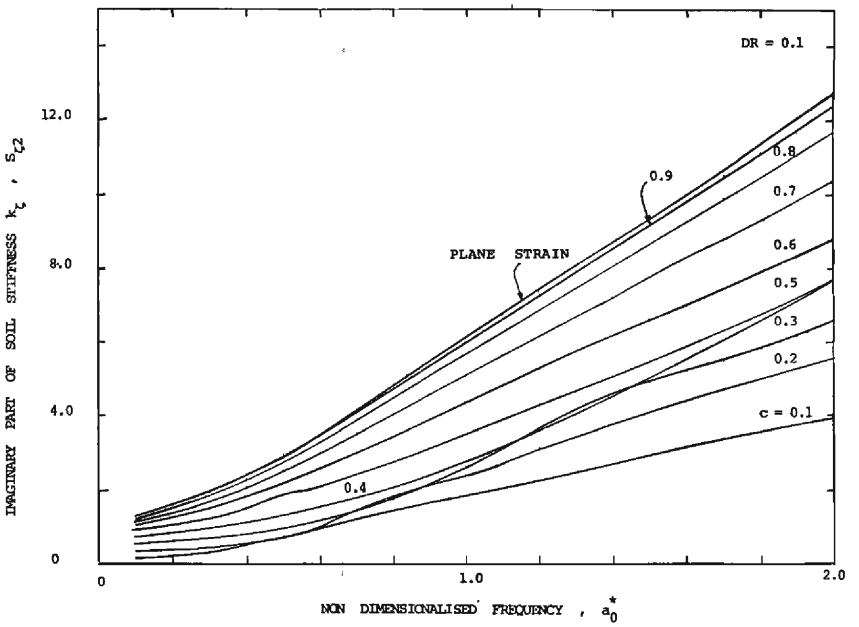


Fig. 10 Imaginary part of soil stiffness in torsion.

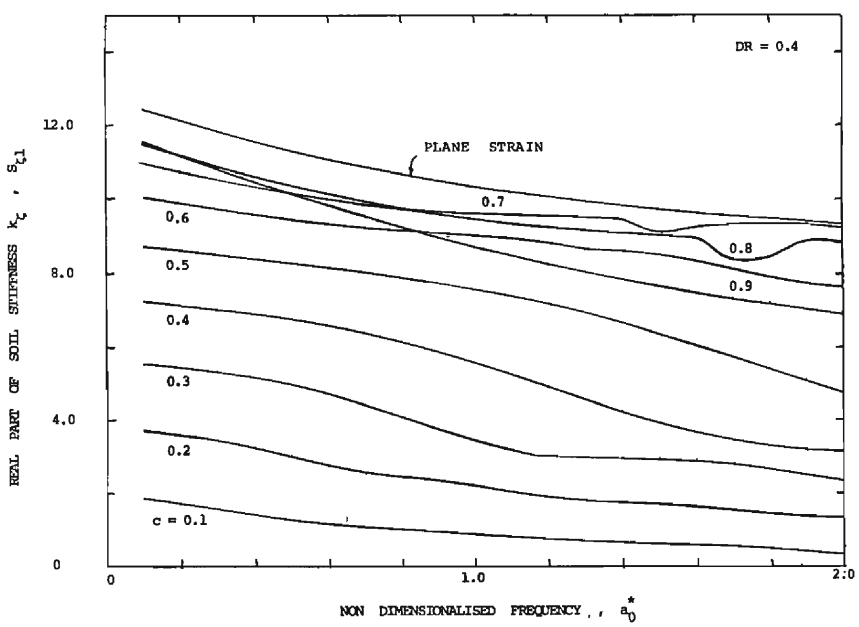


Fig. 11 Real part of soil stiffness in torsion.

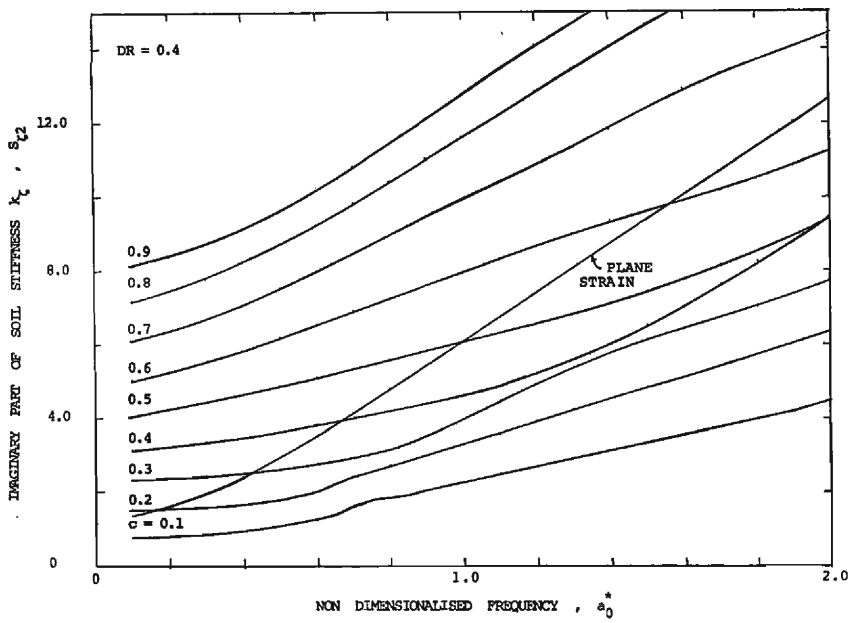


Fig. 12 Imaginary part of soil stifiness in torsion.

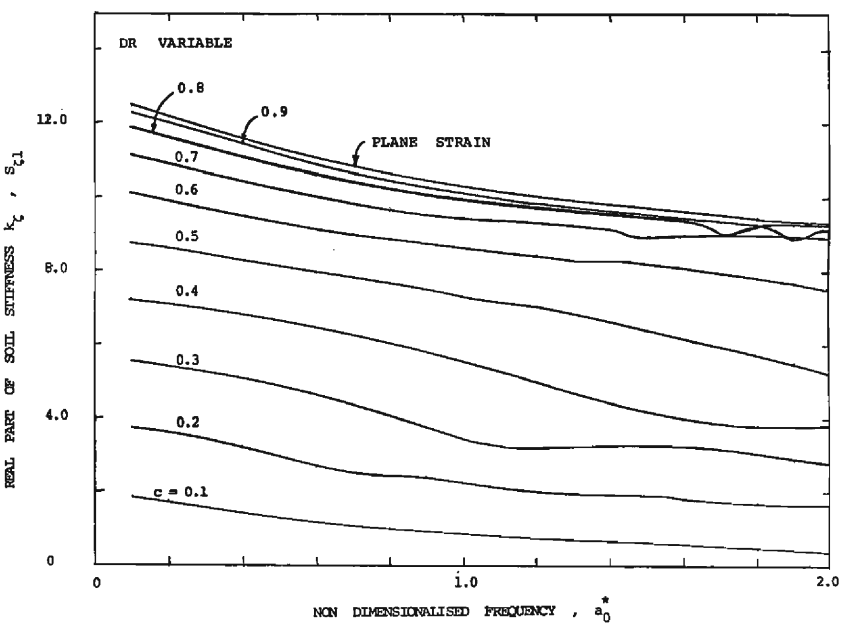


Fig. 13 Real part of soil stiffness in torsion.

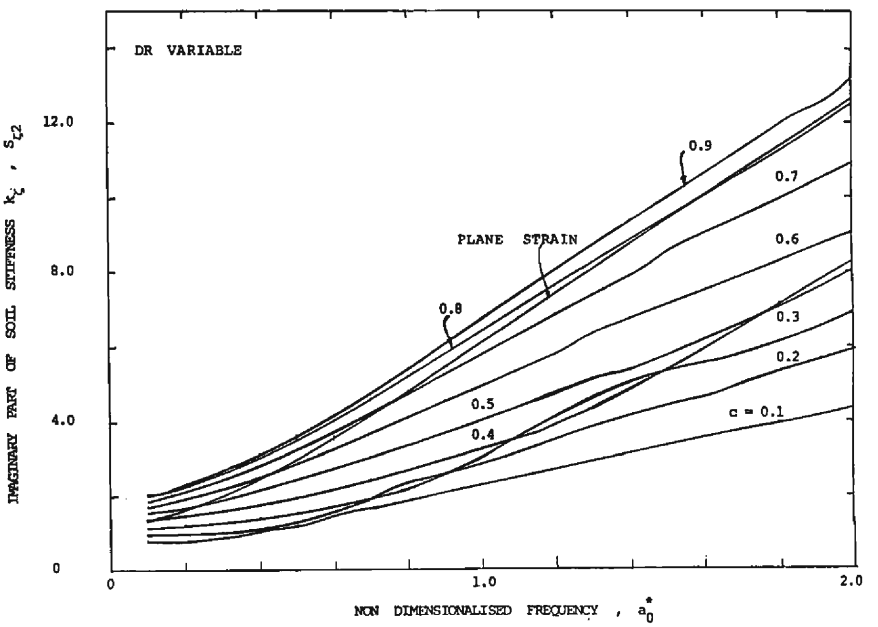


Fig. 14 Imaginary part of soil stiffness in torsion.

## 4. Soil Reactions under Rotational Vibrations (Rocking)

It is assumed in this case that the particles of soil move vertically up and down along the cylinder axis. The motion is un symmetrical as shown in **Fig. 15**. The assumptions are $u=v=\dfrac{\partial w}{\partial z}=0$. The above case is very similar to the vertical case. The forces can be written as (**Fig. 15**)

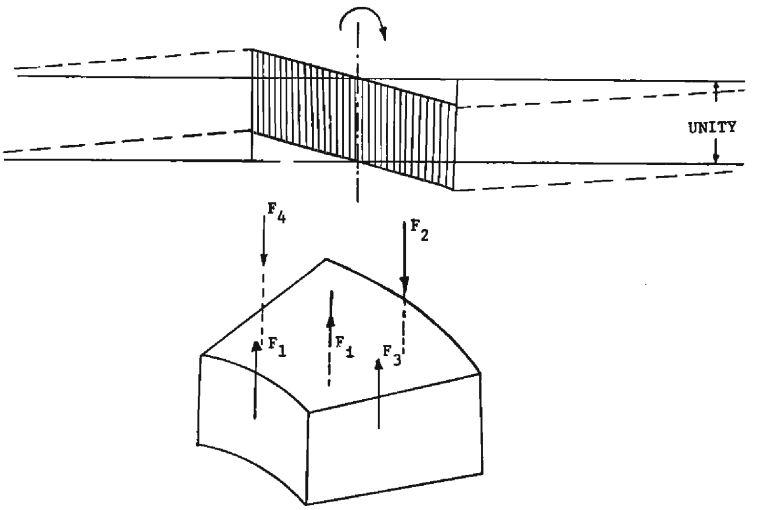


Fig. 15 Soil under rocking vibration.

$$F_1=-G(r)\frac{\partial w}{\partial r}\cdot r\Delta\theta$$

$$F_2=\left(G(r)+\frac{dG(r)}{dr}\Delta r\right)\left(\frac{\partial w}{\partial r}+\frac{\partial^2 w}{\partial r^2}\Delta r\right)(r+\Delta r)\,\Delta\theta$$

$$F_3=-\frac{G(r)}{r}\cdot\frac{\partial w}{\partial\theta}\cdot\Delta r$$

$$F_4=G(r)\left(\frac{1}{r}\frac{\partial w}{\partial\theta}+\frac{1}{r}\frac{\partial^2 w}{\partial\theta^2}\cdot\Delta\theta\right)\Delta r$$

and $$F_i=-\rho(r\Delta\theta\,\Delta r)\frac{\partial^2 w}{\partial t^2}$$

By neglecting higher order terms the equilibrium equation can be written as

$$G(r)\frac{\partial^2 w}{\partial r^2}+\left[\frac{dG(r)}{dr}+\frac{G(r)}{r}\right]\frac{\partial w}{\partial r}+\frac{G(r)}{r^2}\frac{\partial^2 w}{\partial\theta^2}=\rho\frac{\partial^2 w}{\partial t^2} \qquad \cdots\cdots(45)$$

By assuming

$$w=\bar{w}\cos\theta\cdot e^{i\omega t}$$

equation (45) can be transformed to

$$G(r)\frac{d^2\bar{w}}{dr^2}+\left[\frac{dG(r)}{dr}+\frac{G(r)}{r}\right]\frac{d\bar{w}}{dr}-\frac{G(r)}{r^2}\bar{w}=i^2\bar{w}^2\rho\bar{w} \qquad \cdots\cdots(46)$$

By adopting the non-dimensional parameter approach suggested under the vertical case equation (46) can be modified as

$$\left[g\frac{d^2}{d\xi^2}+\left(g'+\frac{g}{\xi}\right)\frac{d}{d\xi}-\frac{g}{\xi^2}-a_0^2\right]\Phi=0 \qquad \cdots\cdots(47)$$

The solution for $\Phi$ can be written as

$$\Phi=\frac{1}{\sqrt{c\xi}}\left[AI_{\sqrt{5}}(z)+BK_{\sqrt{5}}(z)\right] \qquad \cdots\cdots(48)$$

Subjected to the condition that $\bar{w}=r_0$ at a point whose radial and angular co-ordinates are defined by $r=r_0$ and $\theta=0$, respectively, the soil stiffness per unit rotation can be obtained as

$$k_\psi=-\pi r_0^2\cdot G_\infty\left[-0.5\sqrt{c}\left\{AI_{\sqrt{5}}(z_0)+BK_{\sqrt{5}}(z_0)\right\}+a_0\left\{AI'_{\sqrt{5}}(z_0)+BK'_{\sqrt{5}}(z_0)\right\}\right]=G_s r_0^2(S_{\psi 1}+iS_{\psi 2}) \qquad \cdots\cdots(49)$$

The case of rocking vibration has also been studied under three distinct material damping factors as explained under vertical and torsional cases.

The variation of the real and imaginary parts of soil stiffness with $a_0^*$ under rocking are presented in **Fig. 16** to **Fig. 21.** for various values of $c$.

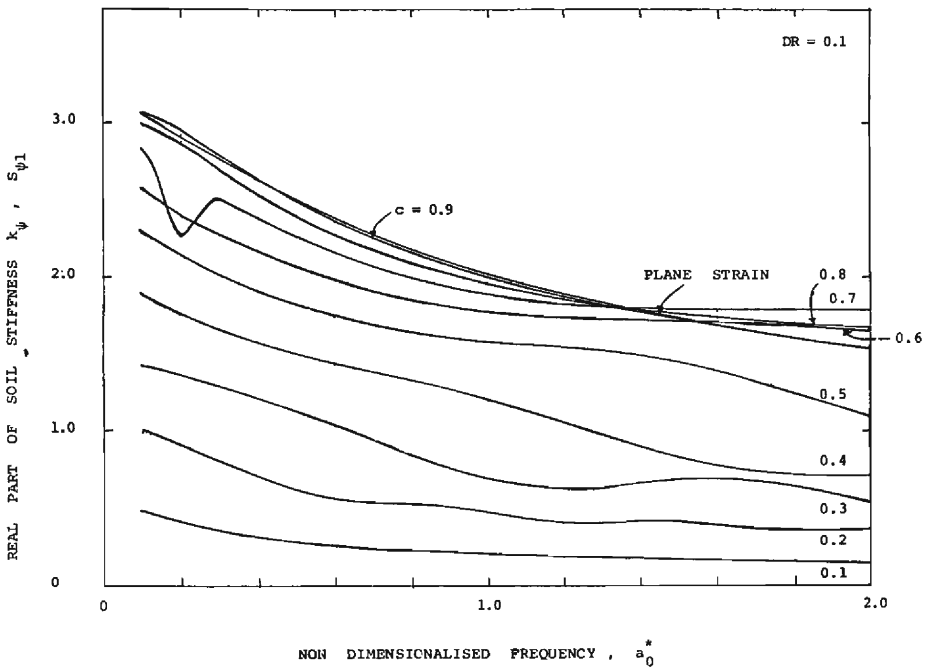


Fig. 16 Real part of soil stiffness in rocking.

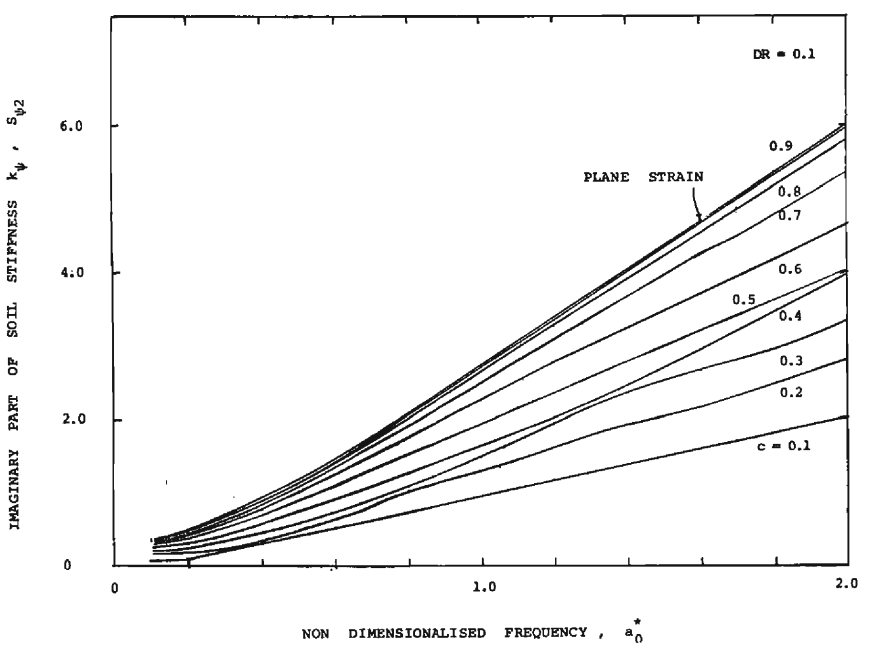


Fig. 17 Imaginary part of soil stiffness in rocking.

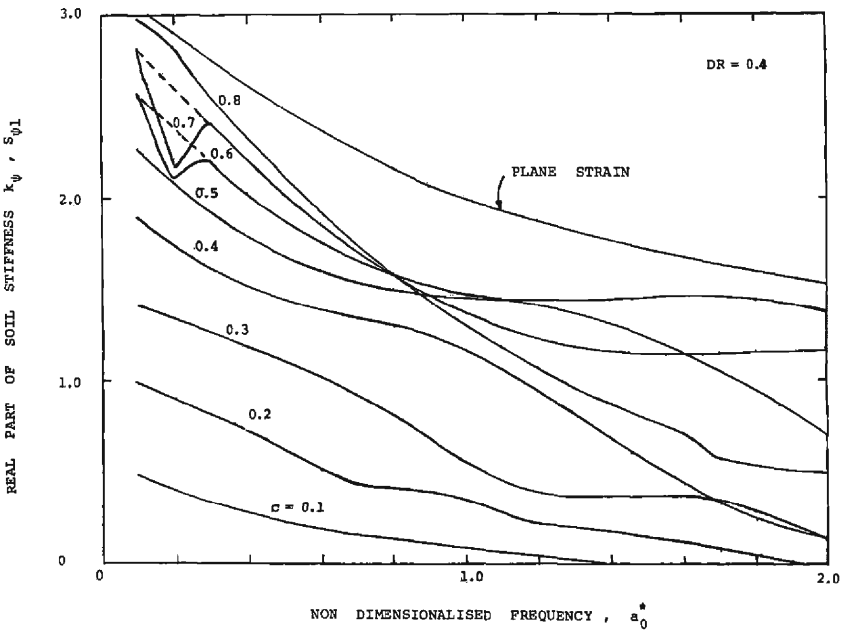


Fig. 18 Real part of soil stiffness in rocking.

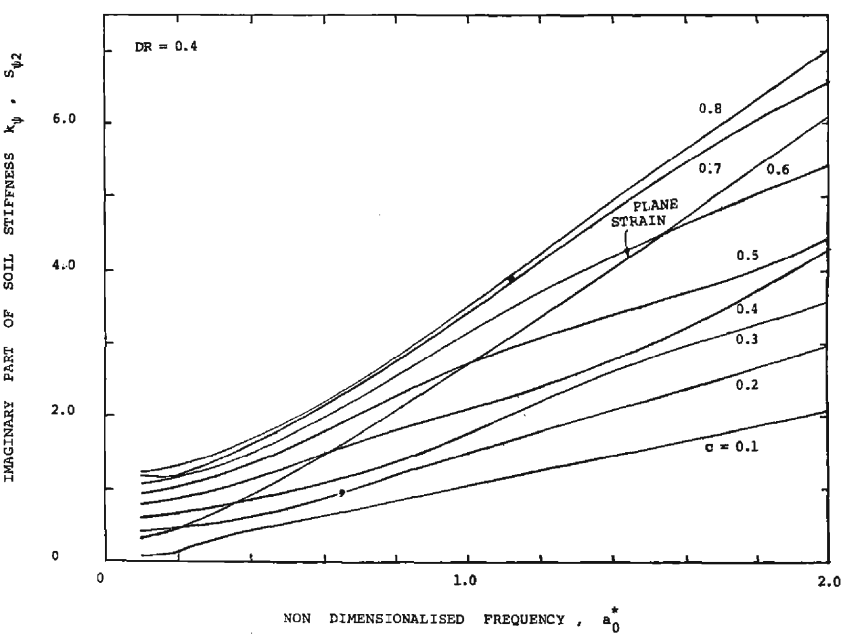


Fig. 19 Imaginary part of soil stiffness in rocking.

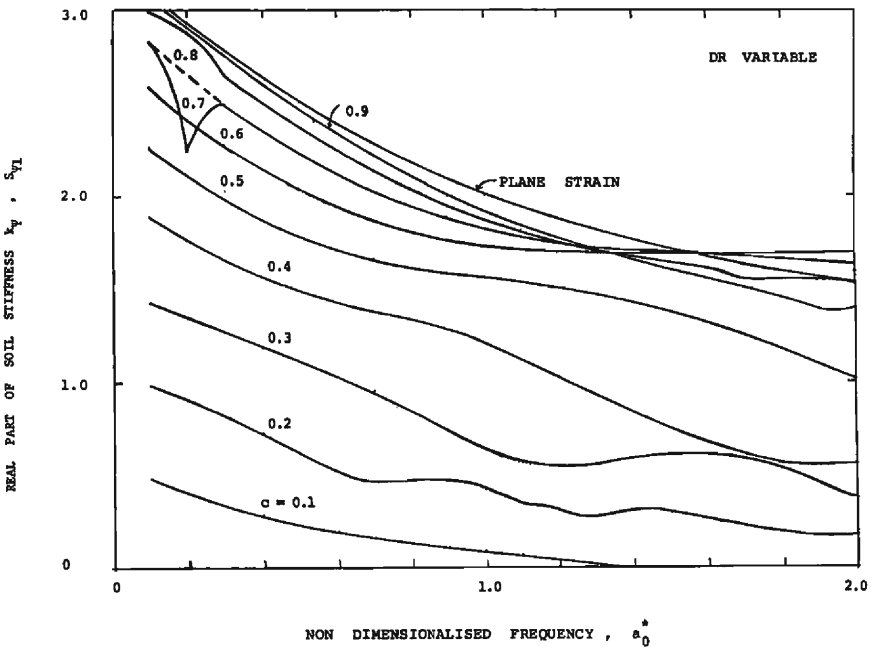


Fig. 20 Real part of soil stiffness in rocking.

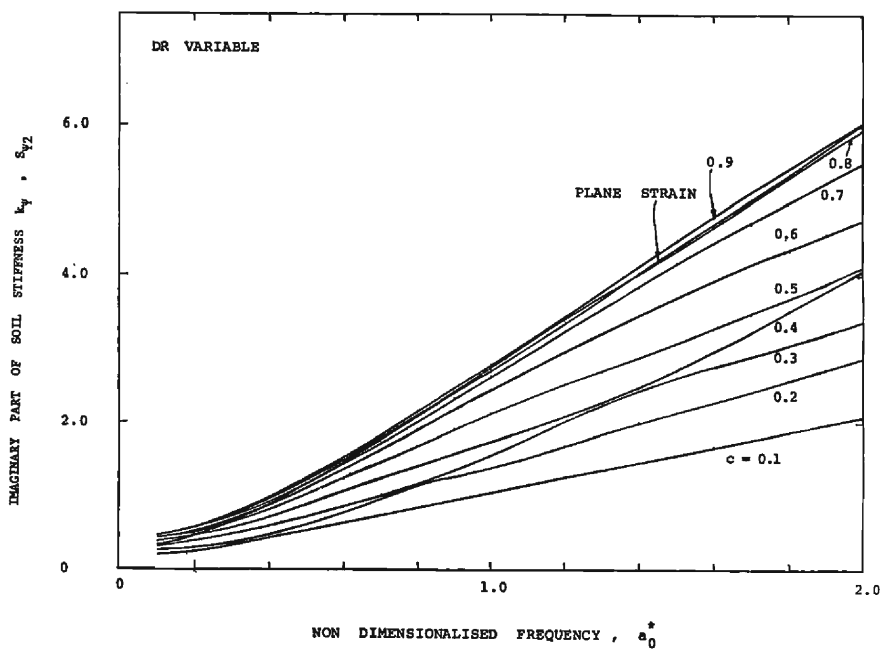


Fig. 21 Imaginary part of soil stiffness in rocking.

## 5. Soil Reactions under Horizontal Vibrations

### 5.1 Variation in $\lambda$ Alone with G Remaining Constant

The soil stiffness under horizontal excitation is far more complicated to derive, in a non-homogeneous soil medium. Only a special case of variation occuring in the Lame's constant $\lambda$, with $G$ remaining constant has been amenable for a closed form solution. Even this case is theoretically more complicated to derive than the other cases dealt herein.

With the assumption that the vertical displacements are negligibly small in comparison to the $u$ and $v$ displacements, the equilibrium equation under horizontal excitation can be written as

$$\frac{\partial \sigma_r}{\partial r}+\frac{\partial \tau_{r\theta}}{r\partial\theta}+\frac{(\sigma_r-\sigma_\theta)}{r}=\rho\frac{\partial^2 u}{\partial t^2} \qquad \cdots\cdots(50)$$

and

$$\frac{\partial \tau_{\theta r}}{\partial r}+\frac{\partial \sigma_\theta}{r\partial\theta}+\frac{2\tau_{\theta r}}{r}=\rho\frac{\partial^2 v}{\partial t^2} \qquad \cdots\cdots(51)$$

where $\sigma_r=\lambda\Delta+2G\dfrac{\partial u}{\partial r}$

$$\sigma_\theta=\lambda\Delta+2G\left(\frac{1}{r}\frac{\partial v}{\partial\theta}+\frac{v}{r}\right)$$

$$\tau_{r\theta}=\tau_{\theta r}=G\left(\frac{\partial u}{r\partial\theta}+\frac{\partial v}{\partial r}-\frac{v}{r}\right)$$

and $\Delta=\left(\dfrac{u}{r}+\dfrac{\partial u}{\partial r}+\dfrac{\partial v}{r\partial\theta}\right)$

With the assumptions that i) only $\lambda$ varies and $G$ remains constant and ii) $u=R\cos\theta\, e^{i\omega t}$ and $v=S\sin\theta\, e^{i\omega t}$ the equilibrium equations given in (50) and (51) can be rewritten as

$$\left[(\lambda(r)+2G)\frac{d}{dr}\left(\frac{1}{r}\frac{d}{dr}(r\cdot)\right)-\frac{G}{r^2}+\rho\omega^2+\frac{d\lambda(r)}{dr}\cdot\frac{d}{dr}+\frac{d\lambda(r)}{dr}\cdot\frac{1}{r}\right]R$$
$$+\left[\lambda(r)\cdot\frac{d}{dr}\left(\frac{1}{r}\cdot\right)+\frac{G}{r}\left(\frac{d}{dr}-\frac{3}{r}\right)+\frac{d\lambda(r)}{dr}\cdot\frac{1}{r}\right]S=0 \qquad \cdots\cdots(52)$$

$$-\left[\frac{(\lambda(r)+G)}{r}\cdot\frac{d}{dr}+\frac{(\lambda(r)+3G)}{r^2}\right]R$$
$$+\left[G\cdot\frac{d}{dr}\left(\frac{1}{r}\frac{d}{dr}(r\cdot)\right)-\frac{(\lambda(r)+2G)}{r^2}+\rho\omega^2\right]S=0 \qquad \cdots\cdots(53)$$

By introducing the potential functions $\phi$ and $\psi$ such that

$$u=\frac{\partial\phi}{\partial r}+\frac{1}{r}\frac{\partial\psi}{\partial\theta}$$

$$v=\frac{1}{r}\frac{\partial\phi}{\partial\theta}-\frac{\partial\psi}{\partial r}$$

and by setting

$$\phi=\Phi\ \cos\theta\ e^{i\omega t}$$

and

$$\psi=-\Psi\ \sin\theta\ e^{i\omega t}$$

where $\Phi$ and $\Psi$ are functions of $r$ alone,

$$R=\frac{d\Phi}{dr}-\frac{\Psi}{r} \qquad \cdots\cdots(54)$$

and

$$S=-\frac{\Phi}{r}+\frac{d\Psi}{dr} \qquad \cdots\cdots(55)$$

it can be shown by differential calculus that the governing equations for the functions $\Phi$ and $\Psi$ may be derived as

$$(\lambda(r)+2G)\left(\frac{d^2\Phi}{dr^2}+\frac{1}{r}\frac{d\Phi}{dr}-\frac{\Phi}{r^2}\right)+\rho\omega^2\Phi=0 \qquad \cdots\cdots(56)$$

and

$$G\left[\frac{d^2\Psi}{dr^2}+\frac{1}{r}\frac{d\Psi}{dr}-\frac{\Psi}{r^2}\right]+\rho\omega^2\Psi=0 \qquad \cdots\cdots(57)$$

As $G$ is assumed to be constant the solution for $\Psi$ can be easily written as

$$\Psi=CI_1(sr)+DK_1(sr) \qquad \cdots\cdots(58)$$

where $s=i\omega/(v_s\sqrt{1+iD_s})$

By adopting a procedure similar to the one described for the vertical case the solution to the function $\Phi$ can be obtained as

$$\Phi=AI_2(z)+BK_2(z) \qquad \cdots\cdots(59)$$

where $z=2b_0\sqrt{\xi/c}$

$b_0=i\omega r_0/(v_p\sqrt{1+iD_s})$

$v_p^2=(\lambda_s+2G_s)/\rho$

$\xi=r/r_0$

$$\lambda_\infty = \lambda_s(1+iD_s)$$

$$\lambda(r_0) = C_1\lambda_\infty$$

$$\lambda(r)+2G_\infty = g(\lambda_\infty+2G_\infty)$$

and $g = c\xi$

Hence the displacements $R$ and $S$ can be written as

$$R = -\frac{b_0}{r_0\sqrt{c\xi}}\left[A\left\{I_1(z)-\frac{2}{z}-I_2(z)\right\}-B\left\{K_1(z)+\frac{2}{z}K_2(z)\right\}\right] - \frac{1}{r}\left[CI_1(sr)+DK_1(sr)\right] \quad \cdots\cdots(60)$$

and

$$S = -\frac{1}{\xi r_0}\left[AI_2(z)+BK_2(z)\right]+C\left[sI_0(sr)-\frac{1}{r}I_1(sr)\right] - D\left[sK_0(sr)+\frac{1}{r}K_1(sr)\right] \quad \cdots\cdots(61)$$

The complex soil stiffness can be obtained by giving unit displacement to the pile, as shown in **Fig. 22.** In addition to the constants $A$, $B$, $C$ and $D$ involved in equations (60) and (61), two additional constants would be involved for establishing continuity of the inner ring with homogeneous visco-elastic, outer soil medium. The six boundary conditions can be written as

i) $u = 1.0$ at $\theta = 0$, $r = r_0$

ii) $v = -1.0$ at $\theta = \pi/2$, $r = r_0$

iii) $u = u_e$ at $\theta = 0$, $r = r_0/c$

iv) $v = v_e$ at $\theta = \pi/2$, $r = r_0/c$

v) $\sigma_r = \sigma_{r,e}$ at $\theta = 0$, $r = r_0/c$

and

vi) $\tau_{r\theta} = \tau_{r\theta,e}$ at $\theta = \pi/2$, $r = r_0/c$

It can easily be understood that with a linear variation of the function, $g$, the homogeneous visco-elastic medium values are obtained at a distance $(r_0/c)$ where $c$ is a fraction. Also it can be shown that the soil reaction is obtained by using the relation

$$P_u = -\int_0^{2\pi}\left(\sigma_r\Big|_{r=r_0}\cdot\cos\theta-\tau_{r\theta}\Big|_{r=r_0}\cdot\sin\theta\right)r_0\cdot d\theta \quad \cdots\cdots(62)$$

from which the complex stiffness is obtained and shown to be equal to

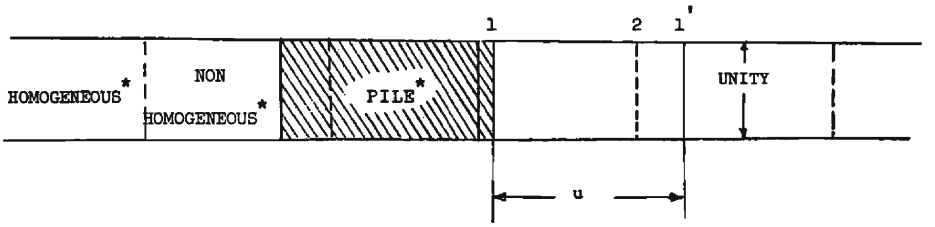


* PRIOR TO DEFORMATION

SECTION

1, 2, 3 PRIOR TO DEFORMATION 1', 2', 3' AFTER DEFORMATION

2, 3 POINTS OF COMPATABILITY

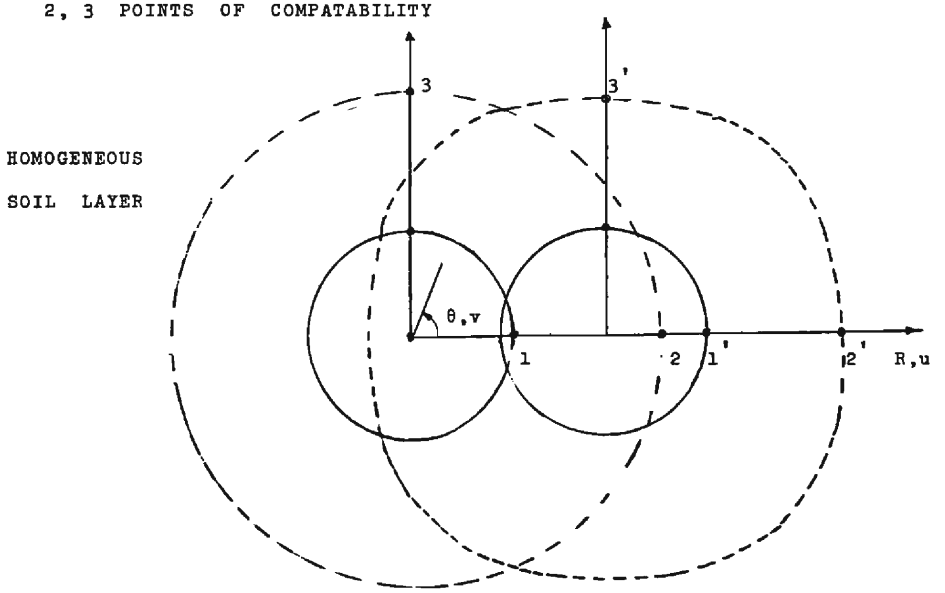


PLAN

Fig. 22 Pile under horizontal loading.

$$k_u = -\pi G a_0^2 \left[ r_0 \left( \frac{dR}{dr} \right)\Big|_{r=r_0} \cdot \left( \frac{1}{b_0'^2} \right) - r_0 \cdot \left( \frac{dS}{dr} \right)\Big|_{r=r_0} \left( \frac{1}{a_0^2} \right) \right] \qquad \cdots\cdots(63)$$

where $b_0'^2 = i^2\omega^2 r_0^2 \rho / [c(\lambda_\infty + 2G_\infty)]$

for the given boundary conditions. The complex soil stiffness, hence can be written as

$$k_u = G_s [S_{u1}(a_0^*, c_1, \nu, D_s, D_R) + iS_{u2}(a_0^*, c_1, \nu, D_s, D_R)] \qquad \cdots\cdots(64)$$

where $\nu$ is Poisson's ratio of the outer soil medium. The values of $S_{u1}$ and $S_{u2}$ can

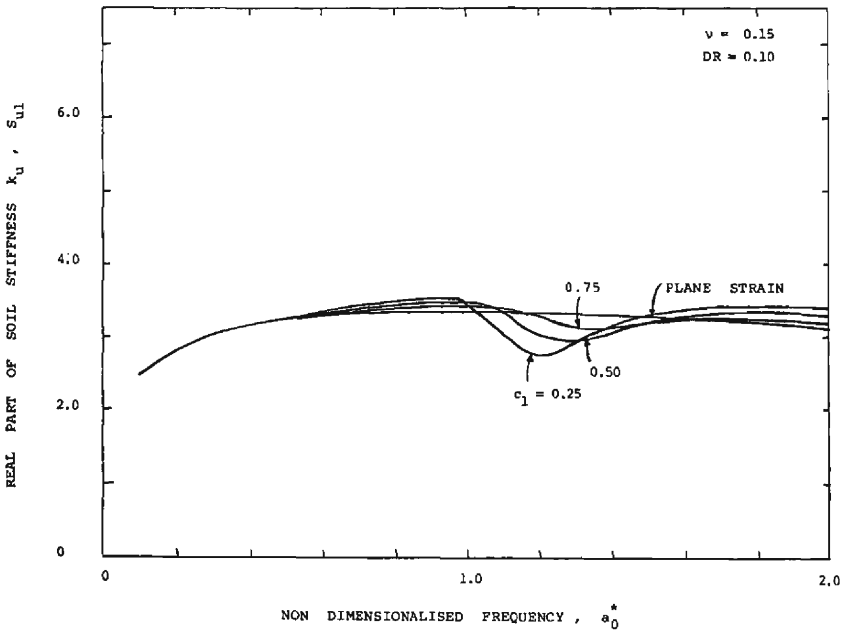


Fig. 23 Real part of soil stiffness in horizontal direction.

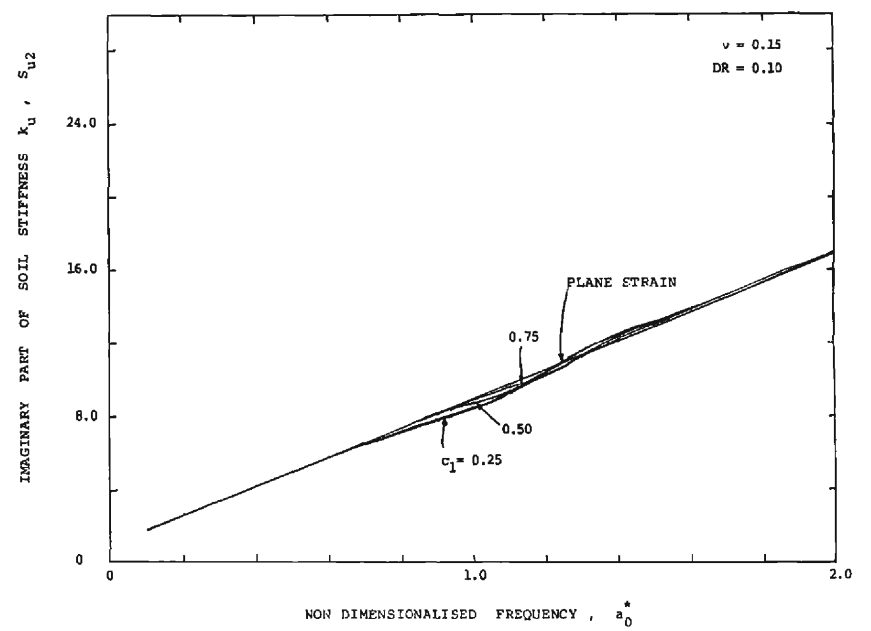


Fig. 24 Imaginary part of soil stiffness in horizontal direction.

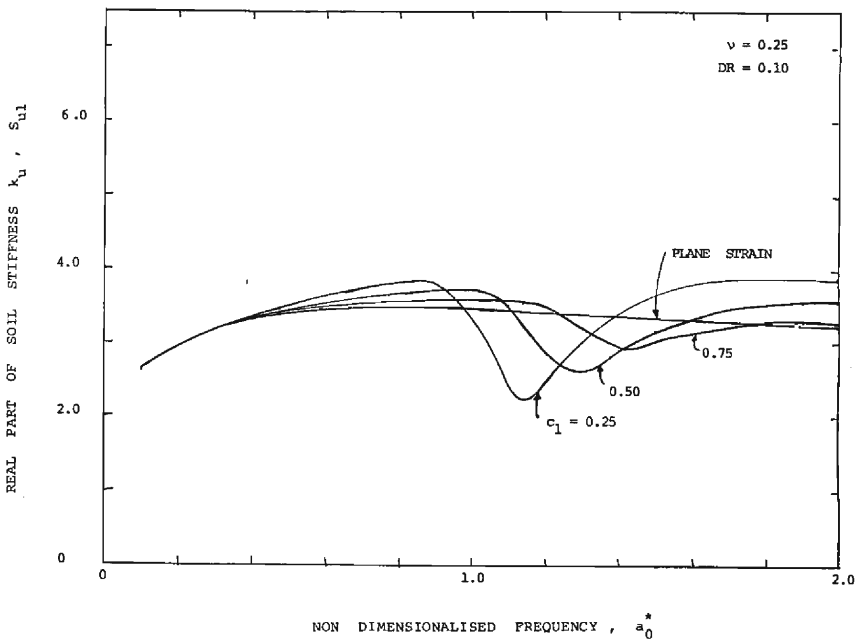


Fig. 25 Real part of soil stiffness in horizontal direction.

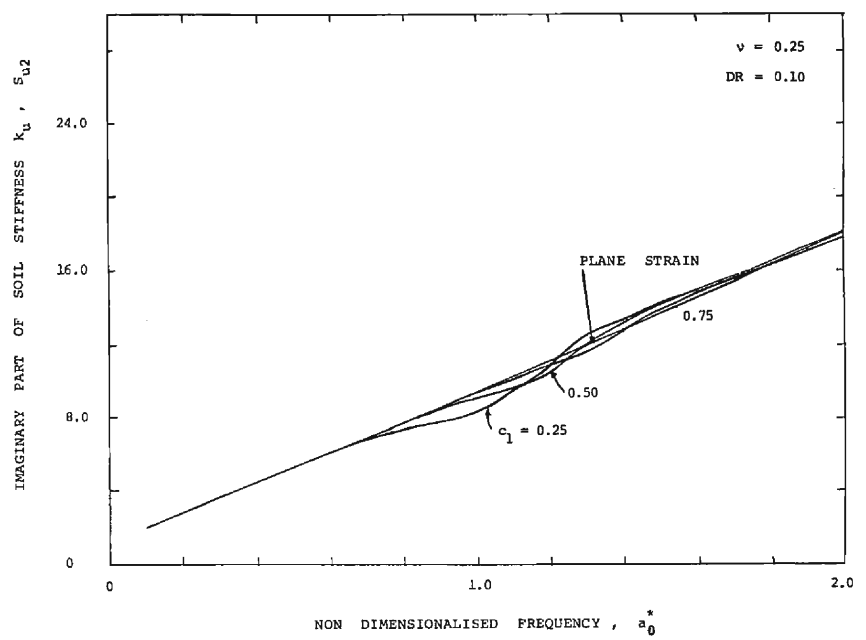


Fig. 26 Imaginary part of soil stiffness in horizontal direction.

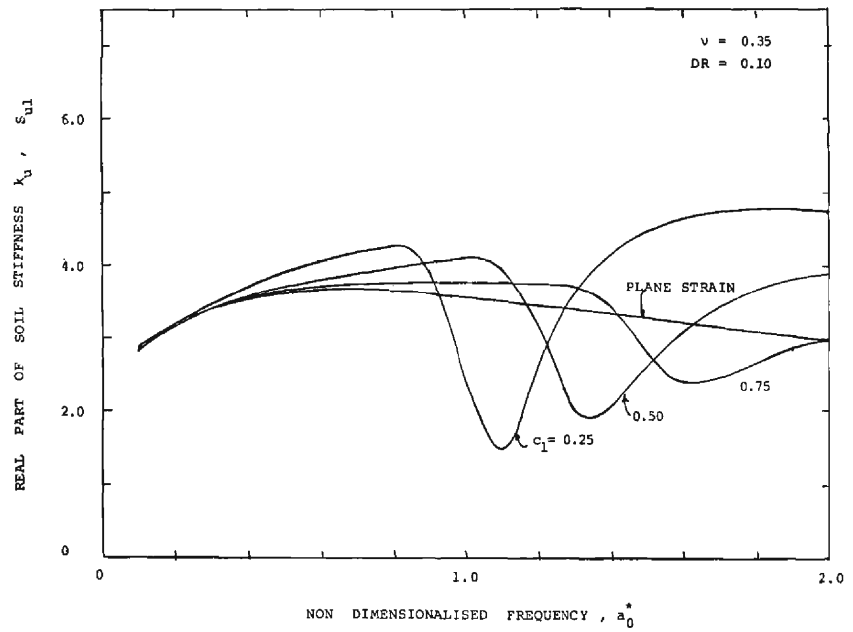


Fig. 27 Real part of soil stiffness in horisontal direction.

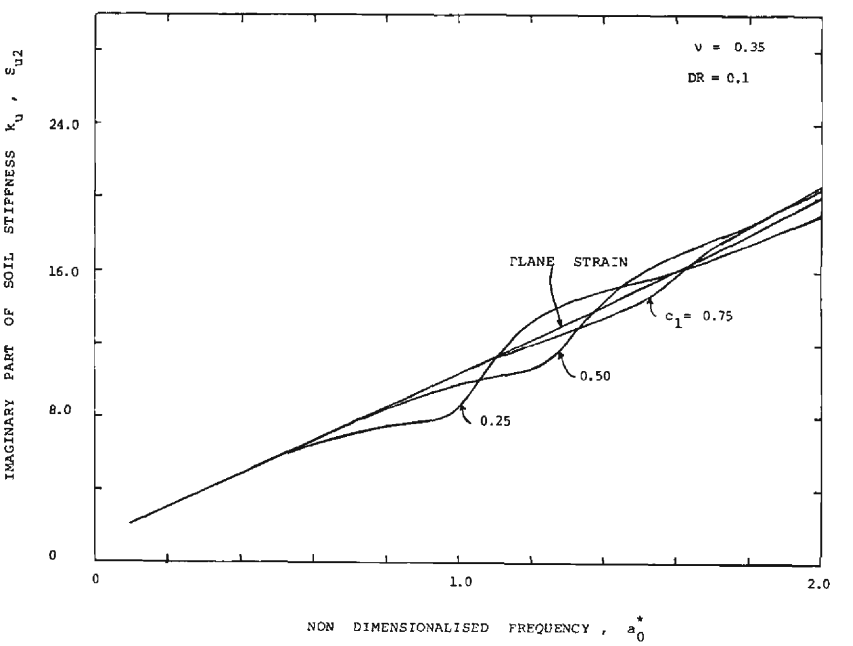


Fig. 28 Imaginary part of soil stiffness in horizontal direction.

be obtained by using computer programmes. Parametric study has been made only for the cases where $D_s=D_R=0.1$. Three values of Poisson's ratio, namely 0.15, 0.25 and 0.35, and three values for the parameter $c_1$, namely 0.25, 0.50 and 0.75 have been included in the parametric study. The value of $c_1$ is defined by the ratio of $\lambda$ at the pile to the value of $\lambda$ at infinite distance from the pile. The plots of $S_{w1}$ and $S_{w2}$ for the cases studied are given in **Fig. 23** to **Fig. 28.**

## 5.2 Approximate Analysis under Horizontal Excitation Including Variations in Both $G$ and $\lambda$

In the absence of a rigorous analytical solution being available under such a case, and also with the knowledge that a linear variation in the soil properties is solvable analytically under the other loading cases, namely vertical, torsional and rocking, the following approximate analysis is suggested.

(i) As in the other cases, assume $g=c\xi$ where $c$ is a fraction. The outer boundary of the non-homogeneous ring is specified by $r=r_0/c$.

(ii) Assume that the inner ring has homogeneous elastic moduli given by $G_R=0.5(1+c)G_\infty$ and $\lambda_R=0.5(1+c)\lambda_\infty$.

For a homogeneous soil medium it is well known that

$$\Phi=AI_1(s_p r)+BK_1(s_p r) \qquad \cdots\cdots(65)$$

and

$$\Psi=CI_1(sr)+DK_1(sr) \qquad \cdots\cdots(66)$$

where

$$s_p=\frac{iw}{v_p\sqrt{1+iD_s}}$$

$$s=\frac{iw}{v_s\sqrt{1+iD_s}}$$

$$v_p=\sqrt{\frac{\lambda_s+2G_s}{\rho}}$$

and

$$v_s=\sqrt{\frac{G_s}{\rho}}$$

Also $R$ and $S$ can be derived as

$$R=A\left[s_pI_0(s_pr)-\frac{1}{r}I_1(s_pr)\right]-B\left[s_pK_0(s_pr)+\frac{1}{r}K_1(s_pr)\right]$$
$$-\frac{1}{r}\left[CI_1(sr)+DK_1(sr)\right] \qquad \cdots\cdots(67)$$

and

$$S=-\frac{1}{r}\left[AI_1(s_pr)+BK_1(s_pr)\right]+C\left[sI_0(sr)-\frac{1}{r}I_1(sr)\right]$$
$$-D\left[sK_0(sr)+\frac{1}{r}K_1(sr)\right] \qquad \cdots\cdots(68)$$

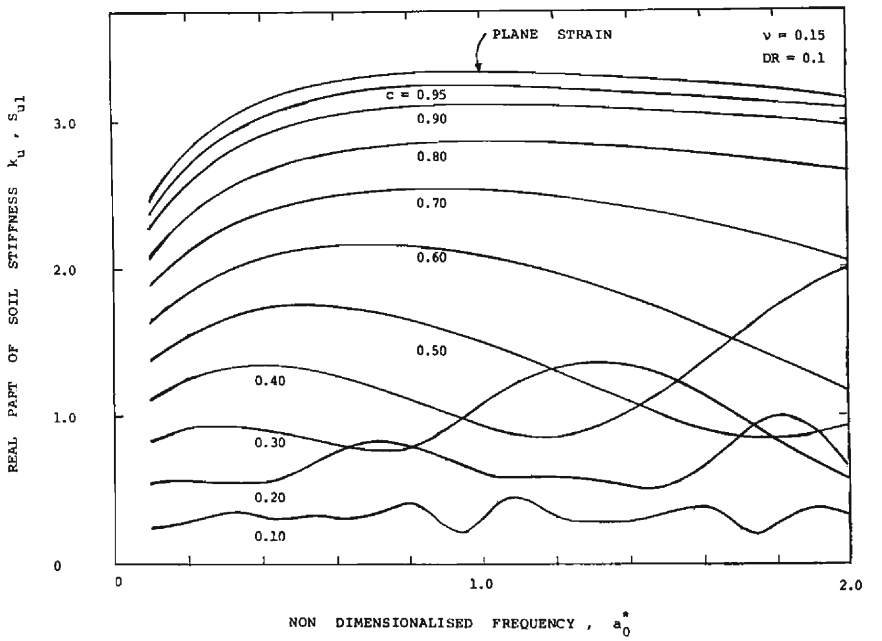


Fig. 29 Real part of soil stiffness in horizontal direction.

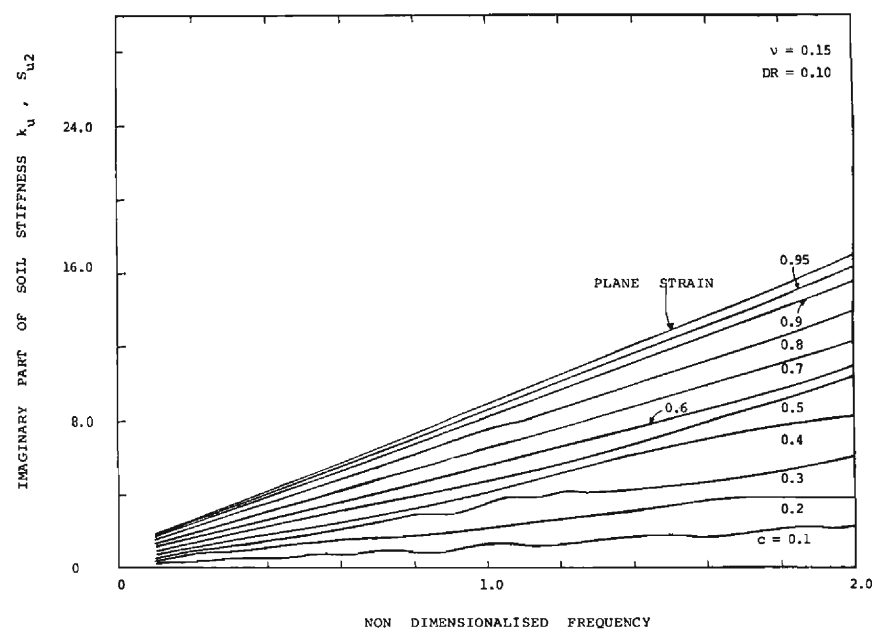


Fig. 30 Imaginary part of soil stiffness in horizontal direction.

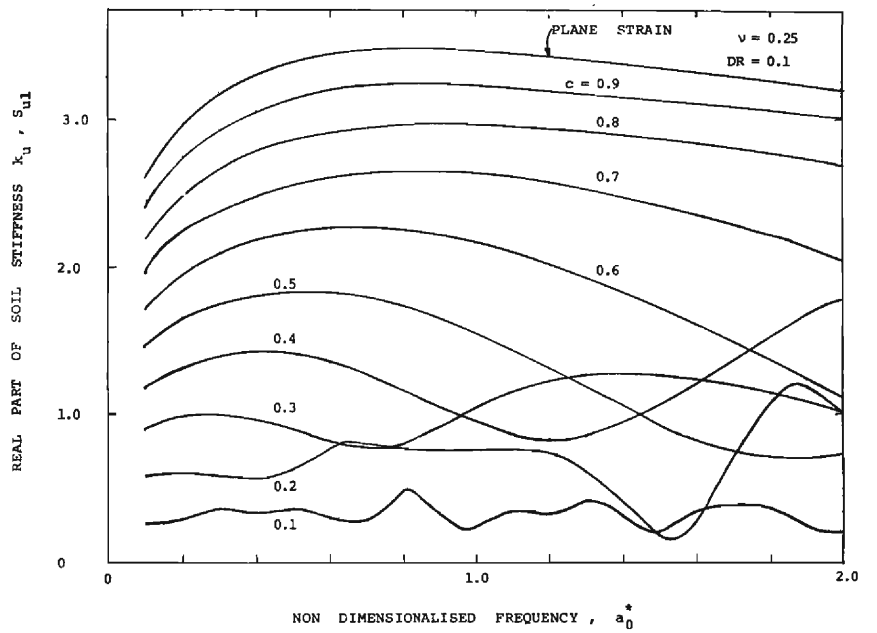


Fig. 31 Real part of soil stiffness in horizontal direction.

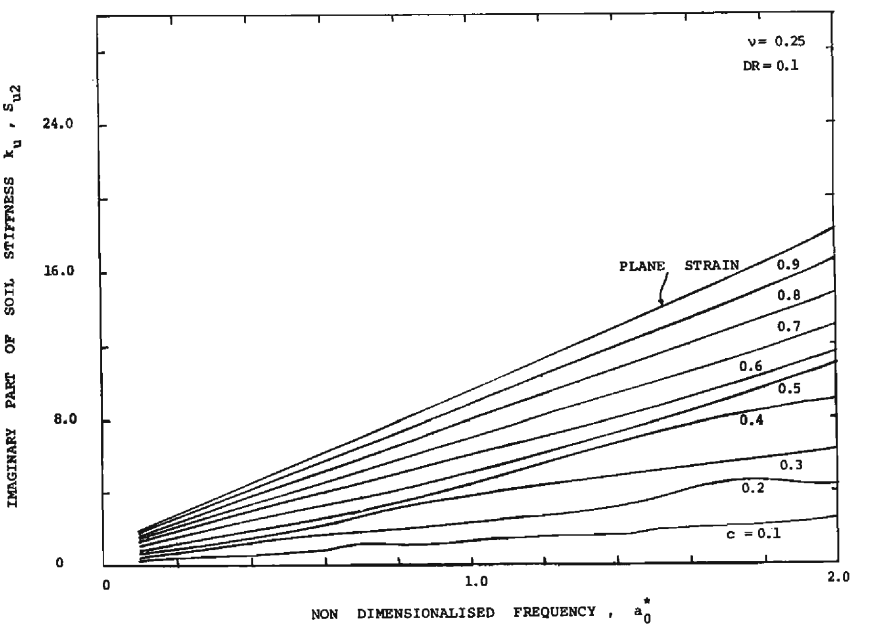


Fig. 32 Imaginary part of soil stiffness in horizontal direction.

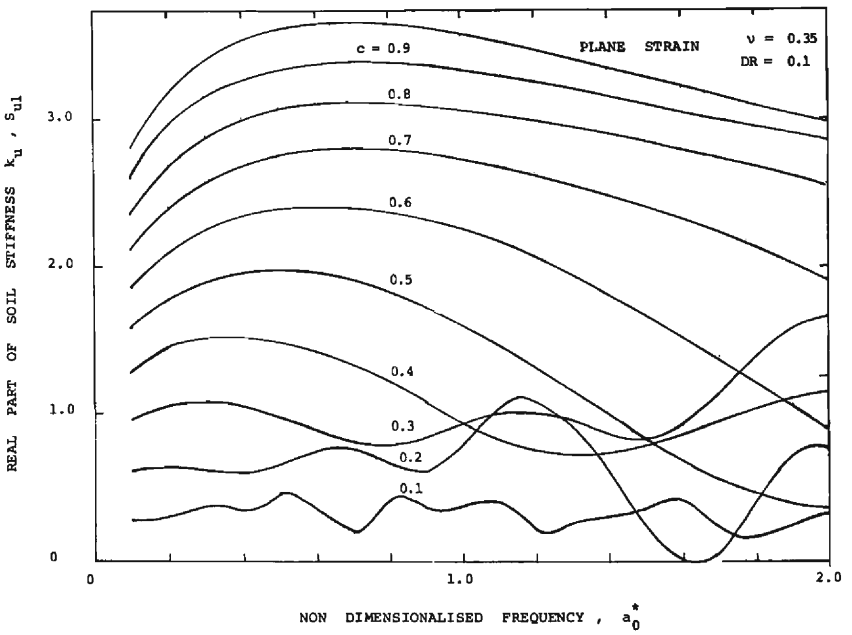


Fig. 33 Real part of soil stiffness in horizontal direction.

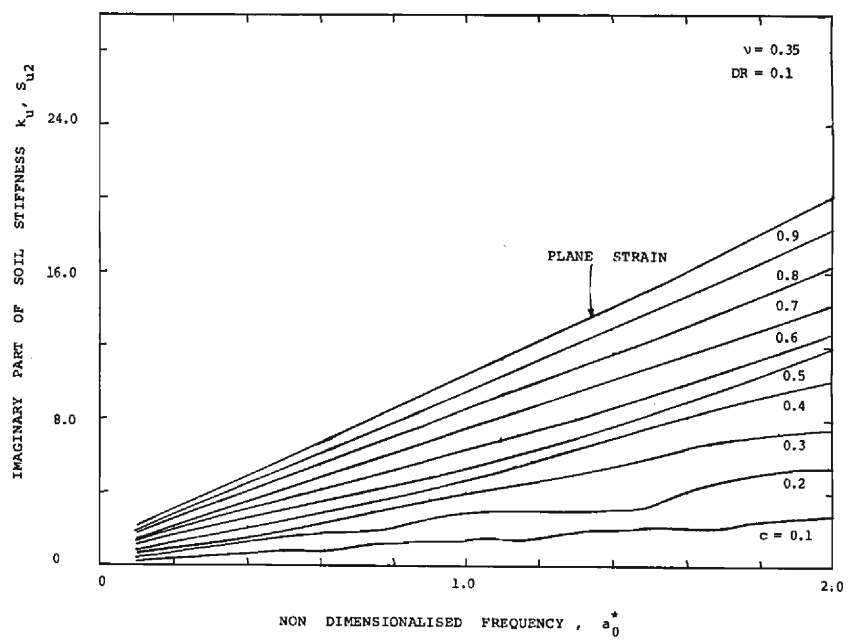


Fig. 34 Imaginary part of soil stiffness in horizontal direction.

Six equations for solving the constants can be written down as explained in the previous case where $\lambda$ alone was varying. Finally the soil reaction due to unit displacement of the pile can be derived using the relation

$$P_u = -\pi c G_\infty \left[ r_0 \frac{dR}{dr}\bigg|_{r=r_0} \cdot \left(\frac{a_0}{b_0}\right)^2 - r_0 \frac{dS}{dr}\bigg|_{r=r_0} \right] \qquad \cdots\cdots(69)$$

By using equation (69) the soil stiffness can be derived as

$$k_u = G_s \left[ S_{u1}(a_0^*,\ c,\ \nu,\ D_s,\ D_R) + i\ S_{u2}(a_0^*,\ c,\ \nu,\ D_s,\ D_R) \right] \qquad \cdots\cdots(70)$$

The real and imaginary parts of soil stiffness so derived are given in **Fig. 29** to **Fig. 34** for values of $D_s = D_R = 0.1$.

## 6. Discussions

### 6.1 General

The study indicates that the dynamic soil reactions are affected to a considerable extent by the radial inhomogeneity in soil medium. Even for a simple case where the variations in the values of $G$ and $(\lambda+2G)$ are assumed as linear considerable shifts from the corresponding plane-strain case values are observed.

### 6.2 Vertical Excitation

In the case of a constant material damping factor for the inner non-homogeneous ring and the outer homogeneous medium, the real part of the complex stiffness is less than the plane-strain values when $c$ is less than 0.5. The real part tends to attain its peak values for values of $c$ around 0.6 and 0.7. As $c$ approaches unity the real and imaginary parts of the stiffness approach those of the plane-strain case indicating the theoretical continuity that is expected between the two cases. However the real part tends to show an oscillating behaviour, very similar to those observed in the case of resonances in soil strata under harmonic excitation. The variations from the mean appear to be considerable for values of $c$ between 0.2 and 0.6. With increasing values of $c$, the inner ring thickness is reduced, and the ring becomes "more stiff". This phenomenon can be easily observed by the shift of the first trough locations as the value of $c$ increases from 0.2 to 0.5. The imaginary part is consistently lower than the corresponding plane-strain values. The damping can be very nearly idealised as hysteretic and viscous dampings, as the variation of $S_{w2}$ is almost linear for all values of $c$.

Considerably lower real parts, and corresponding increases in imaginary parts of the vertical stiffness $S_w$ are observed with an increased material damping factor of 0.4 for the inner ring keeping the damping factor for the outer homogeneous medium

constant at 0. 1. Reduction in $S_{w1}$ and an increase in $S_{w2}$ with increased material damping factor is observed even in the case of plane-strain conditions in a homogeneous soil medium. The important factor to be noted in the behaviours of $S_{w1}$ is that the stiffness falls drastically when the value of $c$ exceeds 0. 6. This behaviour may be due to the pronounced effects of the discontinuity in the material damping factor values between the non-homogeneous and homogeneous soil media. Possibly the thin inner ring under such conditions behaves more like a damper. The fact that considerable increases in values of $S_{w2}$ are observed for values of $c=0.7$ and 0. 8 as can be seen from **Fig. 5** is further evidence.

The behaviour pattern under the cases discussed so far suggest that a realistic value for the material damping factor must depend on the value of $c$. The reasons for a variable material damping factor have already been discussed at length under section. 2.

As can be expected the behaviour shown in **Figs. 6** and **7** is in between the cases with $D_R=0.1$ and $D_R=0.4$. The real and imaginary parts of the soil stiffness converge to the plane-strain values with increase in values of $c$. Also the number of "waves" in the plot of $S_{w1}$ in the frequency range of interest, namely $a_0^*$ varying between 0. 2 and 2. 0, is the same in **Figs. 2, 4** and **6**.

### 6.3 Torsional Excitation

The values of $S_{\zeta 1}$ and $S_{\zeta 2}$ decrease monotonically with decreasing values of $c$ when the material damping factors for the non-homogeneous and homogeneous parts are kept the same at 0. 1. The effects similar to soil resonances are not as pronounced as they were in the case of vertical vibrations. Considerable reduction in the values of $S_{\zeta 1}$ is observed when the material damping factor inside is increased to 0. 4. Remarkable increases in damping as characterised by the values of $S_{\zeta 2}$ are also observed in the frequency range of interest. It was observed by Prof. Novak[2] that the material damping factor contributes significantly to the value of $S_{\zeta 2}$ in the plane-strain case of the homogeneous soil medium at lower non-dimensional frequency parameters. The values of $S_{\zeta 2}$ as plotted in **Fig. 12** indicate the degree to which material damping factor can affect the behaviour. The variable material damping factor leads to more reasonable, and moderate changes as compared to the earlier case. The behaviour shown in **Figs. 13** and **14** is very similar to that observed in **Fig. 9** and **Fig. 10**. The damping can be characterised essentially as viscous with a certain constant value added depending on the material damping factor and the parameter $c$.

### 6.4 Rocking Excitation

Well behaved monotonic decreases in the values of $S_{\phi 1}$ and $S_{\phi 2}$ are observed under all cases of interest in rocking oscillations. More pronounced decrease in $S_{\phi 1}$ and increase in $S_{\phi 2}$, as can be expected now with the knowledge of the behaviour under

vertical and torsional cases, is of course seen in **Fig. 18** and **Fig. 19**, which have a material damping factor of 0.4 for the inner ring. $S_{\psi 2}$ can be considered to a good degree of approximation as viscous damping with hysteretic damping. That is $S_{\psi 2}$ varies linearly with the non-dimensional frequency parameter $a_0^*$. The effect of changes in material damping factor on the constant increases to the value of $S_{\psi 2}$ are less pronounced as compared to $S_{\zeta 2}$.

### 6.5 Horizontal Excitation

A general solution involving variations of both $\lambda$ and $G$ proves to be extremely difficult because of cross coupling between the radial and tangential displacements, and higher order differential equations that result from equations (50) and (51). Hence as a first stage, it is assumed that only $\lambda$ varies and $G$ remains a constant. The variation of $(\lambda+2G)$ is considered linear as expressed in equation (59). Three values for the constant $c_1$, namely 0.25, 0.50 and 0.75 are considered. Similarly, three values of Poisson's ratio considered are 0.15, 0.25 and 0.35, respectively. Marked deviations from the homogeneous, plane-strain stiffness and damping values are noticed for the value of Poisson's ratio equal to 0.35. As Poisson's ratio is decreased, the deviations are also diminished. A phenomenon which can be loosely termed as ring resonance may be the cause for such deviations. The first trough locations, which approximately indicate the possible resonances, shift towards the right with increasing values of $c_1$ in the plots of $S_{u1}$. This is as expected, because a higher value of $c_1$ indicates a lower value for ring thickness, and hence a higher stiffness of the inner ring. The variations in $S_{u2}$ are less marked. However the wavy pattern is maintained in the plots of $S_{u2}$ also.

The plots of $S_{u1}$ and $S_{u2}$ derived from an approximate analysis, in which the variations of $G$ and $\lambda$ are taken into consideration, show remarkable similarity to the plots obtained in the other cases. Both stiffness and damping values increase more or less monotonically with increasing values of the parameter $c$. Three values of Poisson's ratio, namely 0.15, 0.25 and 0.35 have been studied. The influence of soil resonances are significant for values of $c$ up to 0.4, but they tend to diminish later on. The damping, as expressed by $S_{u2}$ can be termed as viscous plus hysteretic as it increases more or less linearly with increasing values of $a_0^*$.

## 7. Conclusions

The effects of radial inhomogeneity in soil arising out of excessive stresses near the pile, soil structure being disturbed while the pile is installed, or any other cause resulting in changes in the soil moduli near the pile location are studied. Expressions have been derived for the dynamic displacements, forces and complex stiffnesses of the pile-soil system. Vertical, torsional, rocking and horizontal excitations have been

studied. Significant deviations are seen between the values obtained in non-homogeneous soil medium and those of the plane-strain case in a homogeneous soil medium. Phenomenon similar to layer resonances in harmonic analysis of soil layers, which can be lossely termed as ring resonances, are observed in the various cases studied. Damping can be closely approximated by viscous and hysteretic dampings for the cases of vertical, torsional, rocking and horizontal excitations. The hysteretic dampings, indicated by the constant additional parts in the imaginary values of complex soil stiffnesses, is significantly increased under torsional excitation when the material damping factor in the non-homogeneous part is increased over that of the outer homogeneous counterpart. In a non-homogeneous soil medium where $G$ is a constant, and $\lambda$ alone varies, only limited variations in the values of $S_{u1}$ and $S_{u2}$ are noticed. The deviations are more pronounced for higher values of Poisson's ratio and lower values of $c_1$. The approximate analysis for horizontal excitation shows behaviour very similar to those of the other cases. Almost monotonic increase in stiffness and damping values, as indicated by $S_{u1}$ and $S_{u2}$, are observed with the increase in value of $c$. The damping of the pile-soil system can be approximated by combined hysteretic and viscous dampings. There is scope for further work in the wave propagation phenomenon in non-homogeneous soil medium, which will go a long way in improving the understanding of the soil-pile interaction problem.

## Acknowledgements

The analytical work reported here-in was carried out while the first author was with the Disaster Prevention Research Institute, Kyoto University, Kyoto, Japan under a UN fellowship (Project No. UNDP/IND/71/120). The help rendered by Mr. Y. Suzuki, Prof. H. Kunieda and Mr. N. Ichikawa of the Disaster Prevention Research Institute in the use of the computer facilities, is gratefully acknowledged. The excellent stenographical and typing assistance provided by Miss K. Oshima in preparing this report is deeply appreciated.

## References

1) Kobori, T., Minai, R., and Baba, K., "Dynamic Interaction Between an Elastic Cylinder and Its Surrounding Visco-Elastic Half-Space", Proceedings, 25th Japan National Congress for Applied Mechanics, Vol. 25, University of Tokyo Press, Tokyo, Japan, 1977, pp. 213-226.
2) Novak, M., Nogami, T., and Aboul-Ella, F., "Dynamic Soil Reaction for Plane Strain Case", EM 4, Journal of the Engineering Mechanics, ASCE, Aug, 1978, pp. 953-959.
3) Novak, M., and Sheta, M., "Approximate Approach to Contact Effects of Piles", Dynamic Response of Pile Foundations: Analytical Aspects, ASCE, Oct., 1980, pp. 53-79.
4) Blaney, G. W., Kausel, E., and Roesset, J. M., "Dynamic Stiffness of Piles", Proceedings of the Second International Conference on Numerical Methods in Geomechanics, June, 1976, ASCE, pp. 1001-1012.
5) Penzien, J., "Soil Pile Interaction", Earthquake Engineering, Prentice Hall Publications, Englewood Cliffs, New Jersey, 1970, pp. 349-381.
6) Tajimi, H., "Earthquake Response of Foundation Structures", Report of the Faculty of

Science and Engneering, Nihon University, 1966, pp. 1. 1-3. 5 (in Japanese).
7) Poulos, H. G., and Mattes, N. S., "The Behaviour of Axially Loaded End Bearing Piles", Geotechnique 19, No. 2, 1969, pp. 285-300.
8) Lakshmanan, N., "Soil-Pile Interaction in Vertical Vibration", GEOT-10-80, Research Report, Faculty of Engineering Science, The University of Western Ontario, Aug., 1980, pp. 1-24.
9) Kobori, T., Minai, R., and Baba, K., "Dynamic Behaviour of a Laterally Loaded Pile", Proceeding of the Specialty Session 10, 9th International Conference on Soil Mechanics and Foundation Engineering, 1977, pp. 175-180.
10) Parmelee, R. A., Penzien, J., Scheffey, C. F., Seed, H. B., and Thiers, G. R., "Seismic Effects on Structures Extending Through Deep Sensitive Clays", Institute of Engineering Research, University of California, Berkeley, Report. SESM 64-2, 1964.
11) Novak, M., "Dynamic Stiffness and Damping of Piles", Canadian Geotechnical Journal, Vol. 11, 1974, pp. 574-598.
12) Kobori, T., Minai, R., and Suzuki, T., "Wave Transfer Functions of Inhomogeneous Viscoe lastic Multi-Layered Media", Annals of the Disaster Prevention Research Institute, Kyoto University, March, 1970, pp. 213-232 (in Japanese).
13) Abramowitz, M., and Stegun, I. A., "Hand Book of Mathematical Functions with Formulas, Graphs, and Mathematical Tables", National Bureau of Standards, Applied Mathematics Series-55, USA, pp. 504-514.
14) Kobori, T., Minai, R., and Suzuki, T., "Dynamic Characteristics of a Layered Sub-Soil Ground", Annals of the Disaster Prevention Research Institute, Kyoto University, April, 1976, pp. 167-217 (in Japanese).
15) Kobori, T., Minai, R., Kusakabe, K., "Dynamic Characteristics of Soil-Structure Interaction System-I", Bulletin of the Disaster Prevention Research Institute, Kyoto University, Vol. 22, Feb., 1973, pp. 111-151.

## Appendix-I

## Notations

$A, B, C, D, E, F$ = constants
$a_0, a_0^*$ = non-dimensional frequency parameters
$b_0, b_0^*, b_0'$ = non-dimensional frequency parameters
$c, c_1$ = constants used to describe non-homogeneous soil medium
$C_0$ = constant
$D_0$ = constant
$D_s, D_R$ = material damping factor of homogeneous soil and non-homogeneous ring, respectively
$F_1, F_2, \cdots F_i$ = elemental forces under different conditions
$G(r)$ = complex shear modulus in the non-homogeneous soil medium
$G_\infty$ = complex shear modulus at infinity of the soil medium
$G_s$ = elastic shear modulus of homogeneous soil medium
$g$ = $G(r)/G_\infty$ or $[\lambda(r)+2G_\infty]/[\lambda_\infty+2G_\infty]$
i = $\sqrt{-1}$
$I_\mu$ = modified Bessel function of the first kind of order $\mu$
$K_\mu$ = modified Bessel function of the second kind of order $\mu$
$k_u$ = complex soil stiffness under horizontal excitation
$k_w$ = complex soil stiffness under vertical excitation
$k_\varphi$ = complex soil stiffness under rotational excitation (rocking)

$k_\zeta$ = complex soil stiffness under torsional excitation
$M$ = Whittaker's characteristic function
$M_{\chi,\mu}$ = Whittaker's function
$r$ = radial co-ordinate
$r_0$ = radius of the pile
$P_u$ = soil reaction under horizontal excitation
$R$ = a function of $r$ describing radial displacement
$S$ = a function of $r$ describing tangential displacement
$S_{u1}$, $S_{u2}$ = real and imaginary parts of non-dimensional complex soil stiffness under horizontal excitation
$S_{w1}$, $S_{w2}$ = real and imaginary parts of non-dimensional complex soil stiffness under vertical excitation
$S_{\varphi 1}$, $S_{\varphi 2}$ = real and imaginary parts of non-dimensional complex soil stiffness under rotational excitation (rocking)
$S_{\zeta 1}$, $S_{\zeta 2}$ = real and imaginary parts of non-dimensional complex soil stiffness under torsional excitation
$t$ = parameter denoting time
$U$ = Whittaker's characteristic function
$u$, $v$, $w$ = displacements in the radial, tangential and vertical directions, respectively
$W_{\chi,\mu}(\epsilon)$ = Whittaker's function
$z$ = vertical co-ordinate
$z$, $z_0$, $z_1$ = modified co-ordinates
$\nu$ = Poisson's ratio
$\Delta r$, $\Delta\theta$ = incremental radial and angular measurements, respectively
$\mu$ = a parameter in Whittaker's function
$\chi$ = a parameter in Whittaker's function
$\xi$ = non-dimensionalised radial co-ordinate
$\eta$ = an intermediate function in the solution process, which is equal to $C_0\left[\xi \frac{d\epsilon}{d\xi}\right]^{-\frac{1}{4}}$ for the horizontal case and $C_0\left[g\xi \frac{d\epsilon}{d\xi}\right]^{-\frac{1}{4}}$ for others
$\theta$ = angular co-ordinate
$\omega$ = circular frequency
$\lambda(r)$ = complex Lamé's constant at a distance $r$
$\lambda_\infty$ = complex Lamé's constant at infinity
$\lambda_s$ = elastic shear modulus of homogeneous soil medium
$\sigma_r$ = radial stress
$\sigma_\theta$ = tangential stress
$\sigma_{r,\epsilon}$ = radial stress corresponding to the plane-strain solution
$\tau_{\theta r}$, $\tau_{r\theta}$ = shear stress
$\tau_{r\theta,\epsilon}$ = shear stress corresponding to the plane-strain solution
$\Phi$ = functions used in Whittaker transformation
$\phi$, $\psi$ = potential functions
$\rho$ = mass density
$\epsilon$ = a function in the solution process which is equal to $4a_0\sqrt{\xi/c}$

## Appendix II

### Expressions for Dynamic Soil Reactions Under Plane-Strain, Homogeneous Conditions[2)]

(a) Vertical:

$$k_w = 2\pi G_s (1+iD_s) a_0 \left[\frac{K_1(a_0)}{K_0(a_0)}\right]$$

(b) Torsional:

$$k_\zeta = 2\pi G_s r_0^2 (1+iD_s) \left[\frac{a_0 K_0(a_0)}{K_1(a_0)}\right]$$

(c) Rocking:

$$k_\varphi = \pi G_s r_0^2 (1+iD_s) \left[1+\frac{a_0 K_0(a_0)}{K_1(a_0)}\right]$$

(d) Horizontal:

$$k_u = \pi G_s a_0^{*2} \cdot T$$

where

$$T = -\frac{4K_1(b_0)K_1(a_0) + a_0 K_1(b_0)K_0(a_0) + b_0 K_0(b_0)K_1(a_0)}{b_0 K_0(b_0)K_1(a_0) + a_0 K_1(b_0)K_0(a_0) + b_0 a_0 K_0(b_0)K_0(a_0)}$$